








Tomato floral induction and flower development are orchestrated by the interplay between gibberellin and two unrelated microRNA-controlled modules

Geraldo F. F. Silva¹, Eder M. Silva¹, Joao P. O. Correa¹ , Mateus H. Vicente² , Nan Jiang³ , Marcela M. Notini¹, Airton C. Junior¹, Frederico A. De Jesus², Pollyanna Castilho¹, Esther Carrera⁴, Isabel López-Díaz⁴ , Erich Grotewold³ , Lazaro E. P. Peres²  and Fabio T. S. Nogueira¹ 

¹Laboratory of Molecular Genetics of Plant Development, Escola Superior de Agricultura 'Luiz de Queiroz' (ESALQ), University of Sao Paulo, 13418-900 Piracicaba, Sao Paulo, Brazil;

²Laboratory of Hormonal Control of Plant Development, Escola Superior de Agricultura 'Luiz de Queiroz' (ESALQ), University of Sao Paulo (USP), 13418-900 Piracicaba, Sao Paulo, Brazil;

³Department of Biochemistry and Molecular Biology, Michigan State University, East Lansing, MI 48824, USA; ⁴Instituto de Biología Molecular y Celular de Plantas, Universidad Politécnica de Valencia (UPV)-Consejo Superior de Investigaciones Científicas (CSIC), Ingeniero Fausto Elío s/n, 46022 Valencia, Spain

Author for correspondence:

Fabio T. S. Nogueira

Tel: +55 19 34294221

Email: ftsnogue@usp.br

Received: 18 July 2018

Accepted: 7 September 2018

New Phytologist (2019) 221: 1328–1344

doi: 10.1111/nph.15492

Key words: flowering time, gibberellin (GA), LANCEOLATE, miR156, miR319, *Solanum lycopersicum*.

Summary

- Age-regulated microRNA156 (miR156) and targets similarly control the competence to flower in diverse species. By contrast, the diterpene hormone gibberellin (GA) and the microRNA319-regulated TEOSINTE BRANCHED/CYCLOIDEA/PCF (TCP) transcription factors promote flowering in the facultative long-day *Arabidopsis thaliana*, but suppress it in the day-neutral tomato (*Solanum lycopersicum*).
- We combined genetic and molecular studies and described a new interplay between GA and two unrelated miRNA-associated pathways that modulates tomato transition to flowering.
- Tomato PROCERA/DELLA activity is required to promote flowering along with the miR156-targeted SQUAMOSA PROMOTER BINDING-LIKE (SPL/SBP) transcription factors by activating SINGLE FLOWER TRUSS (SFT) in the leaves and the MADS-Box gene APETALA1(AP1)/MC at the shoot apex. Conversely, miR319-targeted LANCEOLATE represses floral transition by increasing GA concentrations and inactivating SFT in the leaves and AP1/MC at the shoot apex. Importantly, the combination of high GA concentrations/responses with the loss of SPL/SPB function impaired canonical meristem maturation and flower initiation in tomato.
- Our results reveal a cooperative regulation of tomato floral induction and flower development, integrating age cues (miR156 module) with GA responses and miR319-controlled pathways. Importantly, this study contributes to elucidate the mechanisms underlying the effects of GA in controlling flowering time in a day-neutral species.

Introduction

One key change in meristem identity is at the transition to flowering, where the shoot apical meristem (SAM) transitions to inflorescence (IM) and floral meristems (FM). Five flowering pathways integrate to regulate this transition in the model plant *Arabidopsis thaliana*, including those associated with age and the phytohormone gibberellin (GA) (Andrés & Coupland, 2012). The microRNA156 (miR156) along with its target members of the transcription factor family termed SQUAMOSA PROMOTER BINDING PROTEIN-LIKE (SPL or SBP-box) defines the evolutionary conserved age-dependent flowering pathway (Cardon *et al.*, 1999; Wang *et al.*, 2009; Rubio-Somoza & Weigel, 2011). GA regulates floral transition and flower

initiation under noninductive conditions mostly through nuclear DELLA proteins, a subgroup of GRAS transcription factors family that suppresses GA signaling (Hauvermale *et al.*, 2012; Porri *et al.*, 2012). Low concentrations of bioactive GA lead to the accumulation of DELLA proteins, which delay flowering independent of the photoperiod (Hauvermale *et al.*, 2012). While in long-day (LD) photoperiodic regimes, DELLA proteins repress flowering in leaves and at the SAM, the GA effect on flowering under short-day (SD) conditions is largely restricted to the SAM (Galvão *et al.*, 2012; Porri *et al.*, 2012; Yamaguchi *et al.*, 2014). The molecular basis of *della* mutants remains poorly understood. DELLAs can either activate or deactivate their targets and have genetically separable roles in controlling vegetative development and inflorescence meristem. These observations corroborate with

the observed complex phenotypes of *della* mutants (Serrano-Mislata *et al.*, 2017).

Gibberellin regulates *Arabidopsis* flowering through DELLA interactions with specific miR156-targeted SPLs, including SPL9. The direct interaction with DELLA interferes with SPL9 transcriptional activity and consequently delays floral transition by repressing *MIR172b* and *SUPPRESSOR OF OVEREXPRESSION OF CONSTANS 1* (*SOC1*; Yu *et al.*, 2012). On the other hand, SPL9 recruits DELLA proteins to the *MADS box APETALA1* (*API*) locus, where they induce *API* expression and promote the conversion of lateral primordia into flowers (Yamaguchi *et al.*, 2014). These observations indicate that the interaction between GA and the miR156-SPL/SBP-box module during flowering is more complex than previously anticipated. Indeed, the miR156 targets *SPL3*, *SPL4* and *SPL5*, which positively control floral transition, do not interact with DELLA proteins (Yu *et al.*, 2012), but their transcriptional levels are altered in response to GA at the SAM, independently of miR156 (Galvão *et al.*, 2012).

In addition to the miR156-SPL/SBP module, GA also interacts with the miR319-TCP module during plant development. It has been shown that miR319-targeted *TCPs* positively regulate GA concentrations in both tomato (*Solanum lycopersicum*) and *Arabidopsis* (Yanai *et al.*, 2011). MiR319 targets members of the plant-specific TEOSINTE BRANCHED1/CYCLOIDEA/PCF (*TCP*) family of transcription factors, which contains a conserved noncanonical basic helix–loop–helix domain important for DNA-binding or protein–protein interactions (Cubas *et al.*, 1999). Interestingly, the miR319-TCP module has been implicated in the control of flowering time. Overaccumulation of miR319 leads to downregulation of *Arabidopsis class II TCP* genes, including *TCP4*, and a late-flowering phenotype. By contrast, plants expressing miR319-resistant versions of *TCPs* (or overexpressing *TCPs*) flower earlier (Palatnik *et al.*, 2007; Sarvepalli & Nath, 2011). Recent evidence showed that miR319-targeted *TCP4* binds to *CONSTANS* (*CO*) promoter, therefore inducing *CO* expression and positively regulating photoperiodic flowering (Kubota *et al.*, 2017; Liu *et al.*, 2017). However, miR319-targeted *TCP* genes can also repress target genes in particular developmental contexts (Burko *et al.*, 2013).

Although the use of *Arabidopsis* mutant and transgenic plants altering miRNA-controlled pathways or GA responses has been paramount in understanding the mechanisms underlying floral transition and inflorescence formation, aspects of the flowering time regulation in other species are not fully understood. For instance, it is well known that GAs act positively in the switch to reproductive development in some plants, but negatively in others (King & Ben-Tal, 2001; Boss & Thomas, 2002; Gallego-Giraldo *et al.*, 2007; Wilkie *et al.*, 2008; Gargul *et al.*, 2013; Goldberg-Moeller *et al.*, 2013). The application of bioactive GAs inhibits flowering and flower development in a wide variety of fruit trees. Conversely, the GA inhibitor paclobutrazol (PAC) can promote flowering in apple and pear by reducing bioactive GAs (Pharis & King, 1985; Zhang *et al.*, 2016). While flowering is promoted in the facultative LD *Arabidopsis*, it is inhibited by GAs in the day-neutral tomato (García-Hurtado *et al.*, 2012).

Arabidopsis contains five DELLA proteins (Gallego-Bartolomé *et al.*, 2010), whilst tomato has only one DELLA, called PROCERA (PRO/DELLA). One well-studied recessive *pro* allele contains a point mutation within the VHIID domain (Val (V) to Glu (E) at position 273), which probably reduces PRO/DELLA interaction with targets and thus promotes constitutive GA activity (Bassel *et al.*, 2008). Reduced PRO/DELLA activity delays flowering time in both hypomorphic and null *pro* mutants (Carrera *et al.*, 2012; Livne *et al.*, 2015).

Similarly to *Arabidopsis*, we and others showed that tomato miR156-targeted *SPL/SPB-box* (or *SISBP*s, Salinas *et al.*, 2012) regulates floral transition, probably via floral integrators such as *SINGLE FLOWER TRUSS* (*SFT*, the tomato ortholog of *FLOWERING LOCUS T*, Lifschitz *et al.*, 2006), *FALSIFLORA* (*FA*, a *LFY* ortholog), and *MADS Box* gene *APETALA1/MACROCALYX* (*API/MC*; Zhang *et al.*, 2011; Ferreira e Silva *et al.*, 2014). MiR319-TCP module probably regulates tomato floral transition as well, as plants overexpressing miR319 flower earlier than wild-type (WT) plants (Burko *et al.*, 2013). The effect of miR319 on tomato flowering time may be mediated by the regulation of *SFT* (Burko *et al.*, 2013), though more work is required to support this hypothesis and to uncover which miR319-targeted *TCP* contributes to the control of floral induction in tomato. In addition, it is unknown whether miR156-targeted *SISBP*s regulate tomato flower initiation through an interplay with GA and miR319-targeted *TCP*s.

In this study, we show that age-controlled miR156 integrates with GA and the miR319-targeted *LANCEOLATE* (*LA*), a *TCP4* homolog (Ori *et al.*, 2007; Parapunova *et al.*, 2014), to control tomato flower initiation. The introduction of *pro* allele or GA₃ treatment in tomato miR156-overexpressing plants enhances the delay in floral transition. Strikingly, the introduction of an miR319-resistant allele of *LA/TCP4* in miR156-overexpressing tomato plants abolished canonical flower initiation, whereas it promoted initiation in *Arabidopsis*. Unlike *Arabidopsis*, the expression of the floral integrators *SFT* and *API/MC* is activated by PRO/DELLA, whereas it is repressed by *LA/TCP4*. Our results suggest that the regulation of *SFT* and floral identity genes by the recruitment of age cues via miR156-targeted *SISBP*s and their interactions with GA and the miR319-LA module is the core feature of the mechanisms underlying meristem maturation and floral transition in cultivated tomato.

Materials and Methods

Plant materials and growth conditions

Tomato (*Solanum lycopersicum*) plants were grown in the greenhouse under natural day-length conditions (Lombardi-Crestana *et al.*, 2012). *MIR156*-overexpressing (156-OE), *GA20ox-OE*, *p35S_{pro}:proΔ17*, and *procera* (*pro*) plants in Micro-Tom (MT) or M82 backgrounds were described previously (García-Hurtado *et al.*, 2012; Lombardi-Crestana *et al.*, 2012; Ferreira e Silva *et al.*, 2014; Nir *et al.*, 2017). The *Lanceolate* mutation was introgressed into MT from the original accession LA0335 as previously described (Carvalho *et al.*, 2011). *LANCEOLATE* locus was

PCR-amplified from plants displaying mutant and WT phenotypes and cloned into pENTR d-TOPO (ThermoFisher, Waltham, MA, USA). At least 10 colonies were subjected to sequencing to identify point mutations in the miR319 binding site.

The F₁ hybrid offspring shown in Supporting Information Fig. S9 (see later) was generated by crossing hemizygous 156-OE MT plants with the semidominant *La-1/+* mutant in LA0335 background. *Arabidopsis thaliana* genotypes were in Col-0 and they were grown under LD conditions (16 h : 8 h, light : dark) at 22°C. *Arabidopsis MIR156a*-overexpressing (156-OE) and *tcp4-soj8* plants were described previously (Palatnik *et al.*, 2007; Morea *et al.*, 2016). The F₂ 156-OE; *tcp4-soj8/+* plants were obtained by crossing 156O-E and *tcp4-soj8/+* plants.

Developmental measures

Days post-germination (DPG) were defined by evaluating at least 20 plants for each developmental time point and genotype. The meristem category (vegetative, transition or IM + FM) was defined based on the morphological features depicted in Fig. 1 and in Park *et al.* (2012). The number of leaves to first inflorescence was estimated by counting the leaves produced in the primary shoot when the first flower bud was evident. The time to visible floral buds was set when the first flower bud was visible. Plant height (from the cotyledons to the first inflorescence) was estimated at anthesis. The number of flowers per inflorescence was counted using all the inflorescences in each plant.

Chlorophyll content

At 32 DPG, relative Chl index (Yamamoto *et al.*, 2002) was quantified in fully expanded leaves using a SPAD502 meter (Konica Minolta Optic Inc., Tokyo, Japan).

DNA constructs and plant transformation

We generated SFT-OE MT plants using the *p35S::SFT* construct kindly provided by Dr Lifschitz (Israel Institute of Technology). *p35S::SFT* was introduced into *Agrobacterium tumefaciens* strain GV3101 (pMP90) by electroporation and transferred into cotyledons as previously described (Ferreira e Silva *et al.*, 2014). Transgenic SFT-OE plants at T₃ generation were further used. For protein interaction analyses, ORFs of *SISBP3*, *SISBP15*, *PROCERA/DELLA*, and *LANCEOLATE* were PCR-amplified and subcloned into pENTR d-TOPO (ThermoFisher) and further sequenced. The MiR156-resistant version of *SISBP3* (*rSISBP3*) was made by cloning only the coding region of *SISBP3*, as the miRNA156 site is in the 3'UTR region. For *rSISBP15*, synonymous mutations were inserted into the coding region where the miR156 site is localized (Salinas *et al.*, 2012). For yeast two-hybrid (Y2H) assays, *rSISBP3*, *rSISBP15*, *PROCERA/DELLA*, and *LANCEOLATE* were cloned into pDEST22 (AD) or pDEST32 (BD) (ThermoFisher). For bimolecular fluorescence complementation (BiFC) assays, *rSISBP3*, *rSISBP15*, *PROCERA/DELLA*, and *LANCEOLATE* were cloned into nYFP or cYFP vectors as described. The constructs were delivered into *A. tumefaciens* strain GV3101 (pMP90) by electroporation. The primers used are listed in Table S1.

Yeast two-hybrid and BiFC assays

Yeast two-hybrid assays were performed using the *pJ694-a* strain (James *et al.*, 1996). All genes were fused to both the GAL4 binding domain (BD) and the GAL4 activation domain (AD). Interactions were examined on SD/-Leu/-Trp/-His and SD/-Leu/-Trp/-His/-Ade plates. At least five colonies were evaluated for each combination of proteins. *Nicotiana benthamiana* leaves

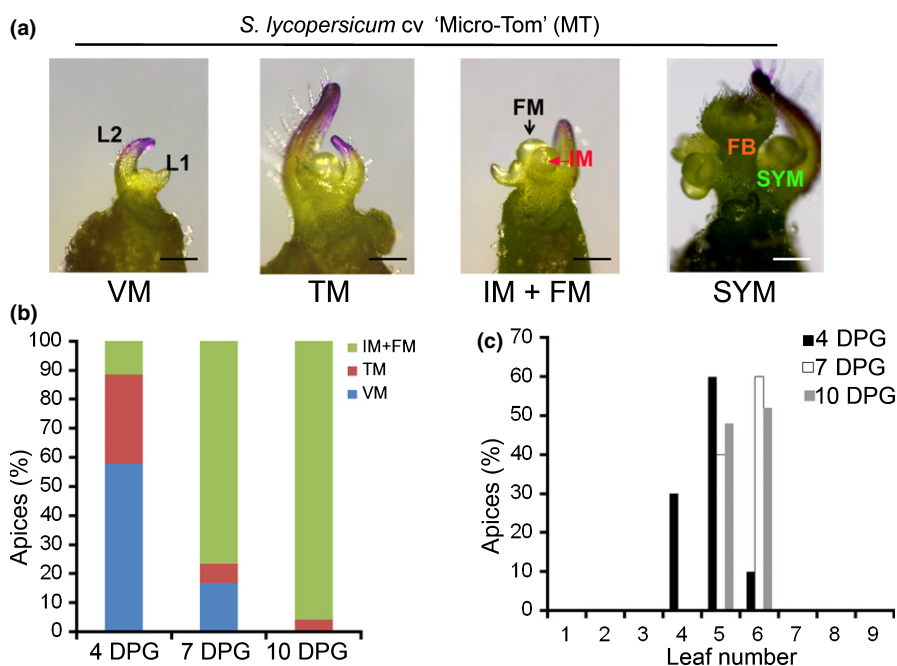


Fig. 1 Four stages of shoot apical meristem (SAM) development in tomato (*Solanum lycopersicum*) cv Micro-Tom (MT). (a) Images of tomato apices showing vegetative meristem (VM), transition meristem (TM), inflorescence plus floral meristem (IM + FM), and sympodial meristem (SYM). IMs and FM meristems are shown by red and black arrows, respectively. FB, floral bud; SYM, sympodial meristem; L, leaf primordium. Bars: VM, TM and IM + FM, 200 µm; FB, SYM, 500 µm. (b) Meristem maturation represented by three sequential stages of maturation of the primary shoot meristem: VM, TM, and IM + FM at 4, 7, and 10 d post germination (DPG) (*n* = 20). (c) Number of leaves formed by the primary shoot meristem from MT plants. Leaves generated by the primary shoot meristem were counted from at least 20 seedlings at each developmental stage (4, 7, and 10 DPG).

were coinfiltrated with *A. tumefaciens* containing nYFP and cYFP vectors harbouring the genes to be tested. The BiFC assay followed the recommendations from Kudla & Bock (2016). The vectors used (nYFP and cYFP) were described in Martin *et al.* (2009).

Hormone treatments and quantification

Gibberellin (GA₃) and PAC (Sigma-Aldrich) were applied to plants by watering. GA₃ treatments (10⁻⁵ M) of WT and 156-OE plants (*n* = 30) were performed from 1 to 10 DPG, and PAC treatments (10⁻⁶ M) of WT (MT), *La-1/+*, 156-OE, and WT (M82) (*n* = 16–57) plants were performed from 1 to 20 DPG. Germination was followed individually to define '1 DPG' (visible hypocotyls hook).

Extraction and quantification of GA₁ and GA₄ were done as described in Martinez-bello *et al.* (2015) using GC-MS. Three biological samples composed of seven 4-DPG apices each were evaluated.

RNA extraction, cDNA synthesis and qRT-PCR analyses

Total RNA was isolated using Trizol reagent (ThermoFisher) according to the manufacturer's instructions, then treated with DNase I (Invitrogen). DNase I-treated RNA (2 µg) was used to generate first-strand cDNA (Varkonyi-Gasic *et al.*, 2007). Reactions were carried out as described in Ferreira e Silva *et al.* (2014) using the StepOnePlus real-time PCR system. Each sample comprised seven apices or the third leaf (for *SFT* expression analyses). Three biological samples with two technical replicates each were used in the quantitative reverse transcription polymerase chain reaction analyses. Expression levels were calculated relative to the housekeeping gene *SITUBULIN* (Mounet *et al.*, 2009) using the $\Delta\Delta C_t$ method (Livak & Schmittgen, 2001). The primers used are listed in Table S1.

Grafting experiments

Tomato plants used as rootstocks were 30-d-old, whereas scions were 20-d-old. At least four replicates were made for each combination of rootstock and scion. The evaluation of flowering was conducted 60 d after grafting. Flowering response was followed in the released lateral shoots of the scions.

Results

Lower *PROCERA/DELLA* and miR156-targeted *SISBP* activities delay meristem maturation and flowering time

Tomato primary shoot is determinate and SAM is completely consumed in the development of the first inflorescence. Therefore, the number of leaves to the first inflorescence in the primary shoot provides a proxy for flowering time (Quinet & Kinet, 2007). To investigate the mechanisms by which GA and microRNA-controlled pathways integrate to modulate transition to flowering in tomato, we analyzed meristem maturation and

flowering time in tomato cv MT (Meissner *et al.*, 2000; Carvalho *et al.*, 2011; Shikata & Ezura, 2016; Vendemiatti *et al.*, 2017). From WT tomato cv MT that consistently initiates five to six leaves before flower initiation (Vicente *et al.*, 2015), we initially characterized meristem maturation in shoot apices at specific developmental stages based on DPG, in which each shoot apex presented large, visible meristem, and surrounding leaf primordia (Fig. 1a). At 4 DPG, almost 90% of the MT shoot apices were at vegetative (VM) and transition meristem (TM) stages, while at 7 or 10 DPG, most of the apices already switched to the reproductive (IM + FM) stage. At 10 DPG, 96% of the shoot apices were at the reproductive developmental stage (Fig. 1b). Most shoot meristems produced between five and six leaves before switching to reproductive growth (Fig. 1c). Given that at 4 DPG most WT shoot apices were at the VM stage (*c.* 60%), and at 10 DPG none of the apices were at the VM stage (Fig. 1b), we focused our further analyses on comparing shoot apices at 4 DPG (vegetative) and 10 DPG (reproductive).

Previously, we showed that temporal modulation of miR156-targeted *SISBP* expression is crucial to control the early stages of flower development (Ferreira e Silva *et al.*, 2014). For instance, *SISBP3* (Solyc10g009080) and *SISBP15* (Solyc10g078700) were differentially regulated during ovary development (Ferreira e Silva *et al.*, 2014) and dynamically expressed during meristem maturation (Park *et al.*, 2012). *Arabidopsis* *SPL3* and *SPL9/SPL15* are homologs of tomato *SISBP3* and *SISBP15*, respectively, and they represent the two main clades of *SPL/SBP*s (VI and VIII, respectively; Preston & Hileman, 2013) that directly regulate the expression of genes associated with floral transition and flower initiation (Wang *et al.*, 2009; Yamaguchi *et al.*, 2009). Therefore, we first evaluated the expression of miR156 and *SISBP3* and *SISBP15* in 4 and 10 DPG apices (Fig. 2a). As expected, miR156 transcript abundances were strongly reduced in the reproductive stage (10 DPG), and *SISBP3* expression increased at a similar developmental stage. Interestingly, *SISBP15* expression was reduced in 10 DPG apices (Fig. 2a). These findings suggested that *SISBP3* and *SISBP15* may function at distinct developmental times of floral transition.

To understand the function of miR156-targeted *SISBP*s during floral transition, we analyzed MT plants overexpressing miR156 (156-OE), in which most *SISBP*s (including *SISBP3* and *SISBP15*) are downregulated (Ferreira e Silva *et al.*, 2014). At 4 DPG, 100% of 156-OE shoot apices were at the VM stage, and at 10 DPG, over 80% of the apices were still at the VM stage (Fig. 2c), in contrast to what was observed in WT apices (Fig. 1b). None of the 10 DPG shoot apices were found at the reproductive developmental stage (Fig. 2c). Like WT shoot apices (Fig. 1c), most 4 DPG 156-OE apices displayed five to six leaf primordia. However, the majority of 10 DPG miR156-overexpressing apices produced nine leaf primordia (Fig. 2d). Given that 50% of 156-OE apices experienced floral transition only at 30 DPG (Fig. S1a), more leaf primordia were continuously produced, reaching *c.* 16 leaves to the first inflorescence. Thus, similarly to *Arabidopsis* (Yu *et al.*, 2012), high levels of miR156 led to delay in tomato flower initiation (Figs 2d, S1b). Nevertheless, the leaf initiation rate did not change in the early stages of tomato

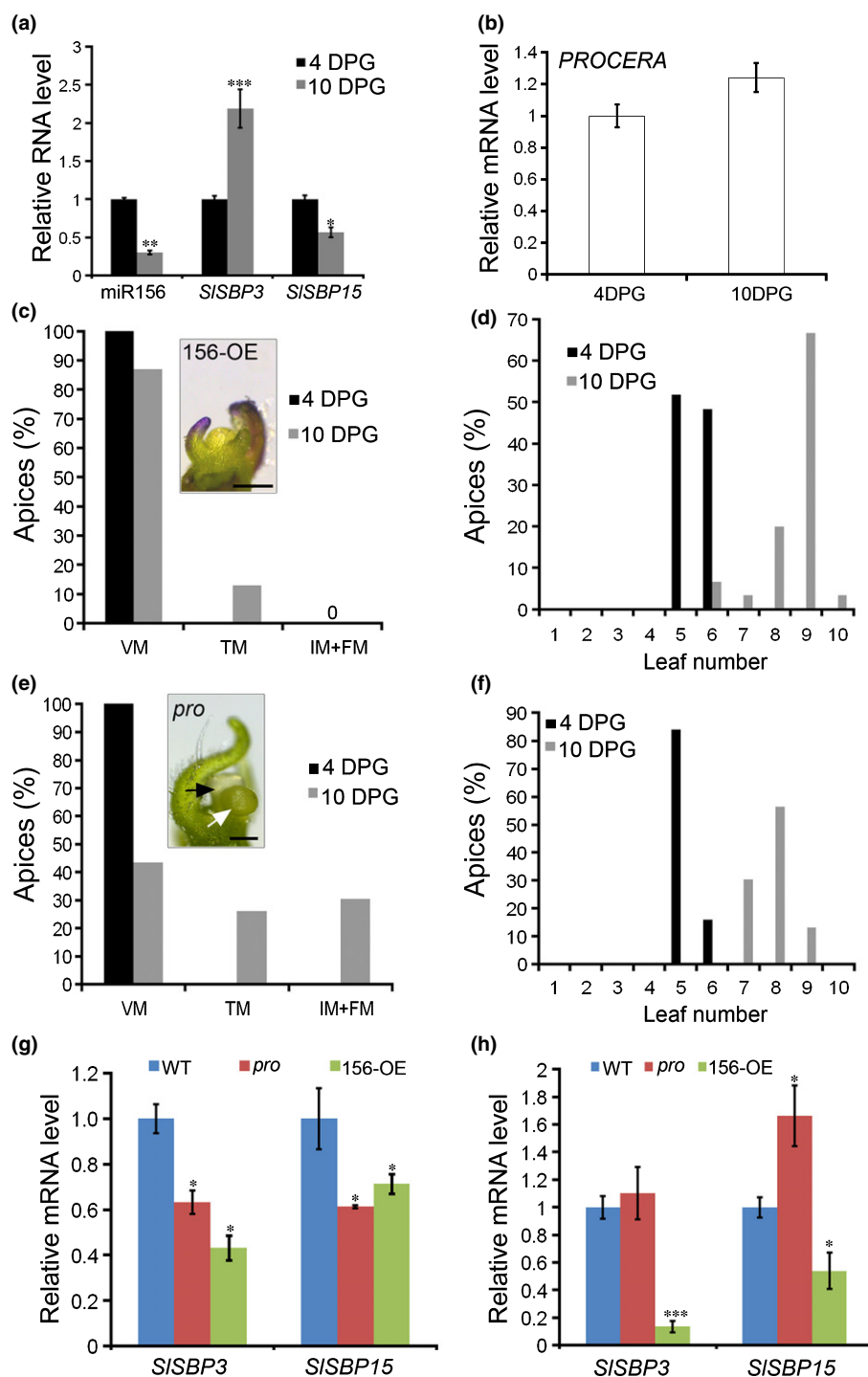


Fig. 2 *PROCERA/DELLA* and miR156-targeted *SISBP3* regulate floral transition and inflorescence development in tomato. (a) Quantitative reverse transcription polymerase chain reaction (qRT-PCR) measurements of the expression of miR156, *SISBP3*, and *SISBP15* in wild-type (WT) shoot apices at 4 and 10 d post germination (DPG) developmental time points. (b) *PROCERA* expression patterns in WT shoot apices at 4 and 10 DPG developmental time points. qRT-PCR experiments shown in (a) and (b) used tissues from 4 DPG apices as reference samples (set to 1.0). (c, e) Meristem maturation represented by sequential stages of maturation of the primary shoot meristem: vegetative meristem (VM), transition meristem (TM), and inflorescence + floral meristem (IM + FM). Meristem maturation was evaluated in 156-OE (c) and *pro* plants (e) ($n = 20$). Insets of representative shoot apices at (c) VM and (e) IM + FM developmental stages are shown. Bars: (c) 200 μ m; (e) 50 μ m. Arrows in (e) indicate FM (black) and IM (white) at the shoot apex. (d, f) Number of leaves formed by the primary shoot meristem from 156-OE (d) and *pro* (f) plants. Leaves generated by the primary shoot meristem were counted from at least 20 seedlings at each developmental stage (4 and 10 DPG). (g, h) Transcriptional levels of *SISBP3* and *SISBP15* in WT, 156-OE, and *pro* shoot apices at 4 DPG (g) and (h) 10 DPG (e). These qRT-PCR experiments used tissues from WT apices as reference sample (set to 1.0). Tomato *TUBULIN* (Solyc04g081490) was used as an internal control for all experiments. qRT-qPCR values are means \pm SE of three biological replicates. Asterisks indicate a significant difference when compared with reference sample according to Student's *t*-test (two tailed): *, $P < 0.05$; **, $P < 0.01$; ***, $P < 0.001$.

meristem maturation (4 DPG), as 156-OE and WT shoot apices showed similar leaf primordia numbers (Figs 1c, 2d).

Resembling 156-OE plants, loss-of-function *PROCERA/DELLA* (Solyc11g011260) mutants show delayed flowering (Carrera *et al.*, 2012; Livne *et al.*, 2015). To better understand the functional role of *PROCERA/DELLA* in flower initiation, we analyzed the *PROCERA* expression pattern during meristem maturation. *PROCERA/DELLA* was similarly expressed in 4 and 10 DPG WT shoot apices (Fig. 2b), suggesting that *PRO/DELLA* is

not transcriptionally regulated during floral transition. Next, we investigated meristem maturation in the hypomorphic *proceral/della* (*pro*) mutant introgressed into MT (Lombardi-Crestana *et al.*, 2012). *pro* harbours a mutation in the *PROCERA/DELLA* gene that lessens protein activity (Bassel *et al.*, 2008; Carrera *et al.*, 2012; Livne *et al.*, 2015). At 4 DPG, 100% of the *pro* shoot apices were at the VM stage (Fig. 2e), similarly to what we observed for 156-OE shoot apices (Fig. 2c). At 10 DPG 40% of the *pro* apices were at the VM developmental stage and *c.* 30% of

the apices switched to the IM + FM stage (Fig. 2e). Comparable to 156-OE apices, the delay in *pro* meristem maturation led to the production of more leaf primordia (seven to nine leaf primordia at 10 DPG; Fig. 2f), in contrast to the five to six leaf primordia produced by the WT (Fig. 1c). Likewise, floral induction was delayed in the *pro* mutant in the M82 background, whereas it was promoted in plants overexpressing the constitutively active stable PRO/DELLA protein (Fig. S2). Taken together, our results indicate that PRO/DELLA activity is required to promote meristem maturation and floral induction in tomato.

To assess whether *pro* late-flowering phenotype (Figs 2, S2; Carrera *et al.*, 2012; Livne *et al.*, 2015) is caused by misregulation of the miR156-*SISBP* module, we evaluated the expression of miR156, *SISBP3*, and *SISBP15* in WT, 156-OE, and *pro* shoot apices. MiR156 transcript abundance did not significantly change in 4 or 10 DPG *pro* apices, but sharply increased in 156-OE, as expected (Fig. S3a). While *PROCERA/DELLA* expression did not change in 156-OE shoot apices, it increased in 4 and 10 DPG *pro* shoot apices (Fig. S3b), suggesting a feedback regulatory mechanism of *PROCERA/DELLA* expression. *SISBP3* and *SISBP15* expression was reduced in 4 DPG *pro* and 156-OE apices (Fig. 2g). At 10 DPG, *SISBP3* and *SISBP15* exhibited a distinct expression pattern: *SISBP3* transcript abundances were similar between WT and *pro*, but they were severely reduced in 156-OE apices. Conversely, *SISBP15* was upregulated in *pro* apices, whereas it was downregulated in 156-OE (Fig. 2h). These observations suggest that *PRO/DELLA* regulates, probably indirectly, *SISBP3* and *SISBP15* at the SAM independently of miR156 (Figs 2, S3). Similar transcriptional regulation of *SPL3*, *SPL4* and *SPL5* by DELLA is observed in *Arabidopsis* SAM (Galvão *et al.*, 2012).

To investigate whether *PRO/DELLA* and miR156-targeted *SISBP*s affect GA homeostasis, we monitored the expression of tomato *GA20-oxidase-1* (*SlGA20ox1*; Solyc03g006880) and *GA2-oxidase-4* (*SlGA2ox4*, Solyc07g061720), which are expressed in apices (Yanai *et al.*, 2011; Livne *et al.*, 2015). *GA20ox* is responsible for the biosynthesis of bioactives GA₁ and GA₄, whereas *GA2ox* catalyzes the deactivation of GA₁ and GA₄ (Fig. S4a; Yamaguchi, 2008). The transcriptional level of *SlGA20ox1* was lower in *pro* apices than in the WT (Fig. S4b), whereas *SlGA2ox4* was upregulated in 4 DPG *pro* apices (Fig. S4c). Our observations are consistent with the possibility that GA homeostasis in *pro* SAM is regulated by a feedback loop (Carrera *et al.*, 2012), in which high GA concentrations/signals suppress GA production via inhibition of *GA20ox* and promote GA catabolism by induction of *GA2ox*. Conversely, the expression of both *SlGA20ox1* and *SlGA2ox4* slightly increased in 4 DPG 156-OE apices (Fig. S4b,c), indicating that miR156-targeted *SISBP*s do not regulate GA homeostasis at the SAM.

Interplay between miR156-*SISBP* module and *PRO/DELLA* regulate floral induction

The *sft* mutant produces a late-flowering phenotype in SD and LD conditions, indicating that *SFT* induces flowering in day-neutral species (Lifschitz *et al.*, 2006). *SFT* was strongly down-

regulated in leaves of both *pro* and 156-OE plants (Fig. S3c), in agreement with their late-flowering phenotype (Fig. 2). At the SAM, tomato genes related to *Arabidopsis* flowering genes such as *FA* (Solyc03g118160) and *API/MC* (Solyc05g056620) are developmentally regulated during meristem maturation (Park *et al.*, 2012) and essential for controlling floral transition and inflorescence development (Molinero-Rosales *et al.*, 1999; Yuste-Lisbona *et al.*, 2016). *FA* transcript abundance did not change in either 4 or 10 DPG *pro* apices, but *FA* was down-regulated in 156-OE apices (Fig. 3a,b). *API/MC* transcripts were not detected at 4 DPG in any genotype, in agreement with a previous report showing detection of *API/MC* transcripts only at the transition and floral meristem stages (Park *et al.*, 2012). At 10 DPG, *API/MC* transcripts were readily detected in WT apices, but they were barely detected in *pro* and 156-OE apices (Fig. 3b), consistent with their late inflorescence development. Importantly, our data indicated that *PROCERA/DELLA* and miR156-targeted *SISBP*s are both required for activating *SFT* expression and, therefore, floral transition. At the SAM, *SISBP*s activate the expression of *FA* whilst *PROCERA/DELLA* and miR156-targeted *SISBP*s activate *API/MC* to promote inflorescence development. Unlike *PROCERA/DELLA*, DELLA REPRESSOR OF GA1-3 (RGA) represses *Arabidopsis* flowering and flower development through *FT* and *MADS-Box* genes (Yu *et al.*, 2012).

Gibberellin promotes *Arabidopsis* flowering through DELLA interactions with miR156-targeted SPLs, mainly SPL9 (a *SISBP15* homolog; Salinas *et al.*, 2012; Yu *et al.*, 2012). Given that both *PROCERA/DELLA* and miR156-targeted *SISBP*s promote flower initiation through similar targets (Figs 3b, S3c), we first tested interactions between *PROCERA/DELLA* and *SISBP3* and *SISBP15* by performing Y2H assays. Neither r*SISBP3* (miR156-resistant version of *SISBP3*) nor r*SISBP15* proteins were able to interact with *PROCERA/DELLA* (Fig. S5). By contrast, a strong interaction was observed when *PROCERA/DELLA* was fused to both GAL4 AD and DNA BD. We also observed a weak interaction when r*SISBP15* was fused to AD and r*SISBP3* to BD (Fig. S5). Next, we checked these interactions by BiFC assay in *N. benthamiana* (Ohad *et al.*, 2007). Neither r*SISBP3* nor r*SISBP15* proteins interacted with *PROCERA/DELLA*, but *PRO/DELLA* interacted with itself. Interaction between r*SISBP15* and r*SISBP3* was also observed by BiFC (Fig. 3c). Our results revealed that *PRO/DELLA* interacts with itself, whilst *SISBP15* and *SISBP3* physically interact in the nucleus, probably to regulate target genes.

Null *pro* alleles lead to male sterility and extremely low female fertility (Livne *et al.*, 2015), which makes it extremely difficult to generate double mutants. Therefore, to further elucidate the interplay between the age-regulated miR156/*SISBP* module and GA responses, we introduced a hypomorphic *pro* allele (Carrera *et al.*, 2012; Lombardi-Crestana *et al.*, 2012) into 156-OE plants to generate 156-OE; *pro* plants. While WT plants consistently produced five leaves before the first inflorescence, *pro* and 156-OE plants initiated around nine and 15 leaves to the first inflorescence, respectively (Fig. 3d). MiR156 overexpression in *pro* (156-OE; *pro*) led to the production of over 20 leaves before flowering (Fig. 3d). As a result, the vegetative architecture was dramatically

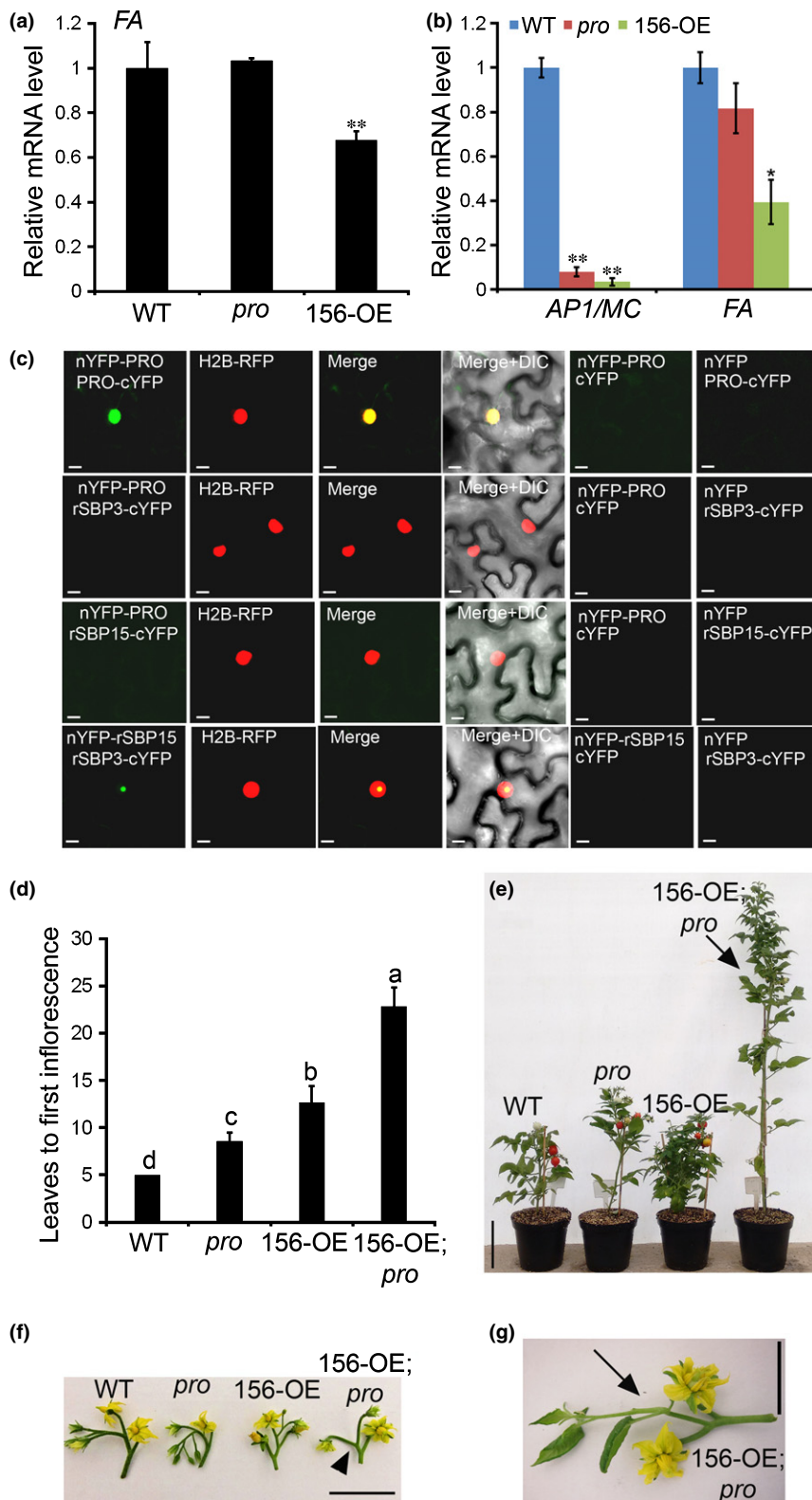


Fig. 3 *PROCERA/DELLA* and miR156-targeted *SISBP*s also function in parallel during floral transition and inflorescence development. (a, b) Comparative expression analyses of: (a) *FALSIFLORA* (*FA*) in 4 d post germination (DPG) apices of wild-type (WT), 156-OE, and *pro*; and (b) *FA* and *APETALA1* (*AP1*)/*MC* in 10 DPG apices of WT, 156-OE, and *pro*. These quantitative reverse transcription polymerase chain reaction (qRT-PCR) experiments used tissues from WT apices as reference sample (set to 1.0). Tomato *TUBULIN* (Soly04g081490) was used as an internal control. qRT-PCR values are means \pm SE of three biological samples. Asterisks indicate a significant difference when compared with reference sample according to Student's *t*-test (two-tailed): *, $P < 0.05$; **, $P < 0.01$. (c) Bimolecular fluorescence complementation experiments using *Nicotiana benthamiana* leaves infiltrated with agrobacteria. The combinations of nYFP-PRO with cYFP, nYFP with PRO-cYFP, nYFP with rSBP3-cYFP, nYFP with rSBP15-cYFP, and nYFP-rSBP15 with cYFP were used as negative controls. Histone 2B (H2B)-RFP was used as a nuclear marker. The corresponding differential interference contrast (DIC) image combined with merged image (Merge + DIC) is also shown. The yellow color in the merged images indicates colocalization between coexpressed proteins. (d) Flowering time in WT, *pro*, 156-OE, and 156-OE; *pro* plants (mean \pm SD; $n = 12$). Distinct letters indicate significant difference according to Student's *t*-test ($P < 0.001$). (e) Representative WT, *pro*, 156-OE, and 156-OE; *pro* plants used for flowering time analysis. (f) Representative inflorescences of WT, *pro*, 156-OE, and 156-OE; *pro* plants. Arrowhead shows the reduction of inflorescence complexity in the first inflorescence of 156-OE; *pro* plants. (g) Representative image of 156-OE; *pro* primary inflorescence, indicating partial vegetative reversion (arrow). Bars: (c) 10 μ m; (e) 8 cm; (f, g) 4 cm.

changed in 156-OE; *pro* plants (Fig. 3e), and inflorescence branching was reduced (less flowers per inflorescence; arrowhead in Fig. 3f). Additionally, we often observed leaf branches in place of flower branches inside the 156-OE; *pro* inflorescences (arrow in Fig. 3g), suggesting reversion of some FM to VM. Both

modifications in the 156-OE; *pro* inflorescence architecture are probably a result of prolonged downregulation of flowering identity genes, which altered meristem maturation. Given that our *pro* is a hypomorphic (weak) mutant and that miR156 overexpression does not completely abolish *SISBP* expression (Ferreira e

Silva *et al.*, 2014), it is possible the additive effects observed in 156-OE; *pro* plants are partially caused by the combination of two weak genetic effects in the same pathway. That null *pro* alleles generate obligatory parthenocarpic plants (Livne *et al.*, 2015) and the fact that there are no available null alleles of *SISBP*s preclude us from testing this idea at this point. Despite these limitations, our observations indicate that PROCERA/DELLA regulates tomato flowering partially through modulating *SISBP* expression (Fig. 2g), as well as by acting in parallel with miR156-targeted *SISBP*s to regulate flowering target genes (Fig. 3).

To further substantiate our findings, we crossed *GA20ox-OE* plants (which show high levels of bioactive GAs and delayed flowering time; García-Hurtado *et al.*, 2012) with 156-OE plants. As anticipated, 156-OE; *GA20ox-OE* plants produced more leaves to the first inflorescence than 156-OE and *GA20ox-OE* plants (Fig. 4a), supporting the additive effect of the miR156/*SISBP* module and GA in regulating floral induction. Likewise, 156-OE plants treated with gibberellic acid (GA_3) for 10 DPG initiated more leaves to the first inflorescence (Fig. 4c). The application of GA_3 for 10 DPG also delayed flowering time and meristem maturation in M82 and MT plants (Fig. 4b,d), further supporting the idea that high GA concentrations/responses delay tomato flower initiation.

MiR319-targeted *LANCEOLATE* represses meristem maturation and floral induction

MiR319-targeted *TCP4* (the closest homolog of *LANCEOLATE*) promotes photoperiodic flowering in *Arabidopsis* (Kubota *et al.*,

2017; Liu *et al.*, 2017). To investigate whether miR319-targeted *LANCEOLATE* regulates floral transition in tomato, we initially measured the transcript abundances of miR319 and *LA* in 4 and 10 DPG WT apices. MiR319 transcripts accumulated at higher levels in 10 DPG apices, whereas *LA* transcript abundances were reduced (Fig. S6a). Comparable *LA* expression pattern was observed during meristem maturation in tomato cv M82 (Fig. S6b). This suggests that miR319 may be important to dampen *LA* expression during floral transition and early inflorescence development. Next, we introgressed the semidominant *La* mutation from the accession LA0335 (<http://tgrc.ucdavis.edu>) into MT as previously described (Carvalho *et al.*, 2011). We identified a single nucleotide substitution (G to T/U) in the 3'-end of the miR319-recognition site of the *LA* gene in the mutant MT plants. Such mutation generated an miR319-resistant *LA* allele, the same as identified in the *La-1* allele described by Ori *et al.* (2007). Thus, the *La* mutant introgressed into MT was hereafter referred to as *La-1* (Fig. S6c).

To investigate meristem maturation and flowering time in the *La-1* mutant, we first inspected the apices of homozygous (*La-1/La-1*) and heterozygous (*La-1/+*) mutant plants. *La-1/La-1* seedlings displayed an odd meristem that produced very few leaf primordia and, as a result, the seedlings were not viable at later developmental stages (Fig. S6d). *La-1/+* plants presented a WT-like meristem (Fig. 5a) and were viable, and therefore selected for further experiments. *La-1/+* shoot apices at 4 DPG presented 100% of VM (Fig. 5a), similarly to *pro* and 156-OE apices (Fig. 2). At 10 DPG, no *La-1/+* shoot apices were at the IM + FM stage (Fig. 5a), comparable to 10 DPG 156-OE apices

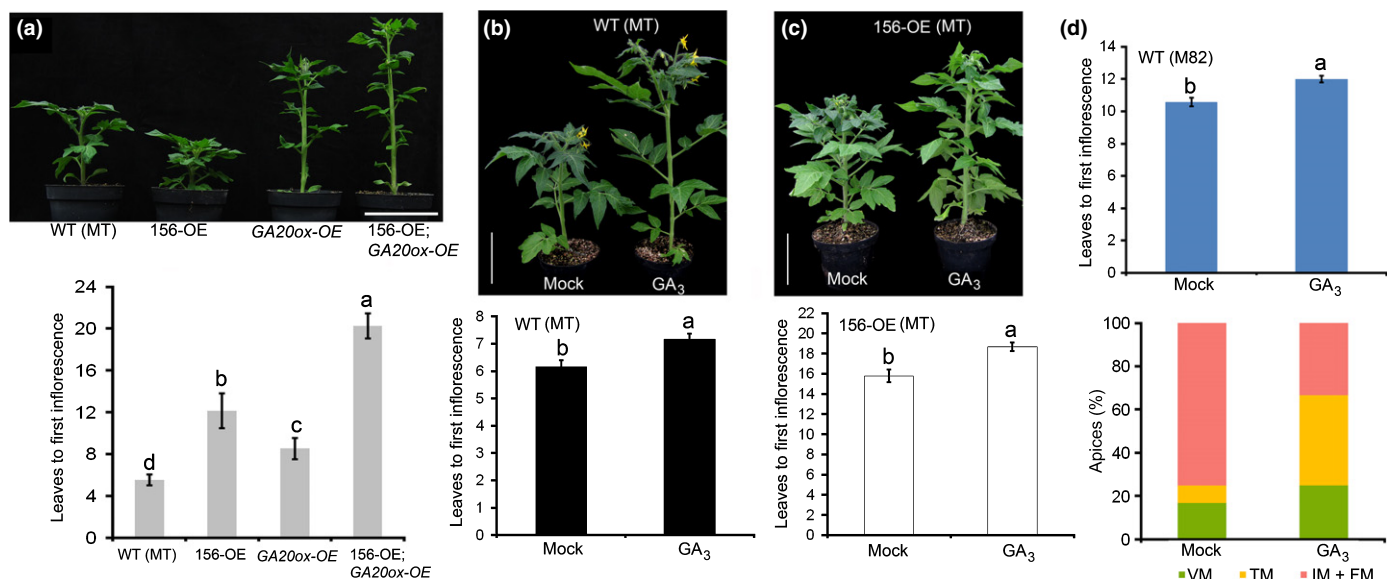


Fig. 4 High GA concentrations/responses delay tomato floral transition. (a) Representative wild-type (WT) cv Micro-Tom (MT), 156-OE, *GA20ox-OE*, and 156-OE; *GA20ox-OE* plants and flowering time (measured by leaves to first inflorescence) (mean ± SD; $n = 12$). Distinct letters indicate significant difference according to Student's *t*-test ($P < 0.05$). (b–d) Gibberellin (GA) responses of WT cv MT (b), miR156-overexpressing cv MT (156-OE) (c), and WT cv M82 plants (d). (b, c) Representative WT and 156-OE cv MT plants (upper panels) and flowering time (measured by leaves to first inflorescence) of plants watered with GA_3 or ethanol (mock) for 10 d post-germination (lower panels) (mean ± SD; $n = 30$). (d) Flowering time (measured by leaves to first inflorescence) of WT cv M82 plants watered with GA_3 or ethanol (mock) for 10 DPG (upper panel) (mean ± SD; $n = 10$). Meristem maturation of WT cv M82 represented by three sequential stages of maturation: vegetative meristem (VM), transition meristem (TM), and inflorescence plus floral meristem (IM + FM) in mock and GA_3 treatments (lower panel). GA_3 treatment delayed M82 meristem maturation. Distinct letters indicate significant difference according to Student's *t*-test ($P < 0.01$). Bars: (a) 7 cm; (b, c) 8 cm.

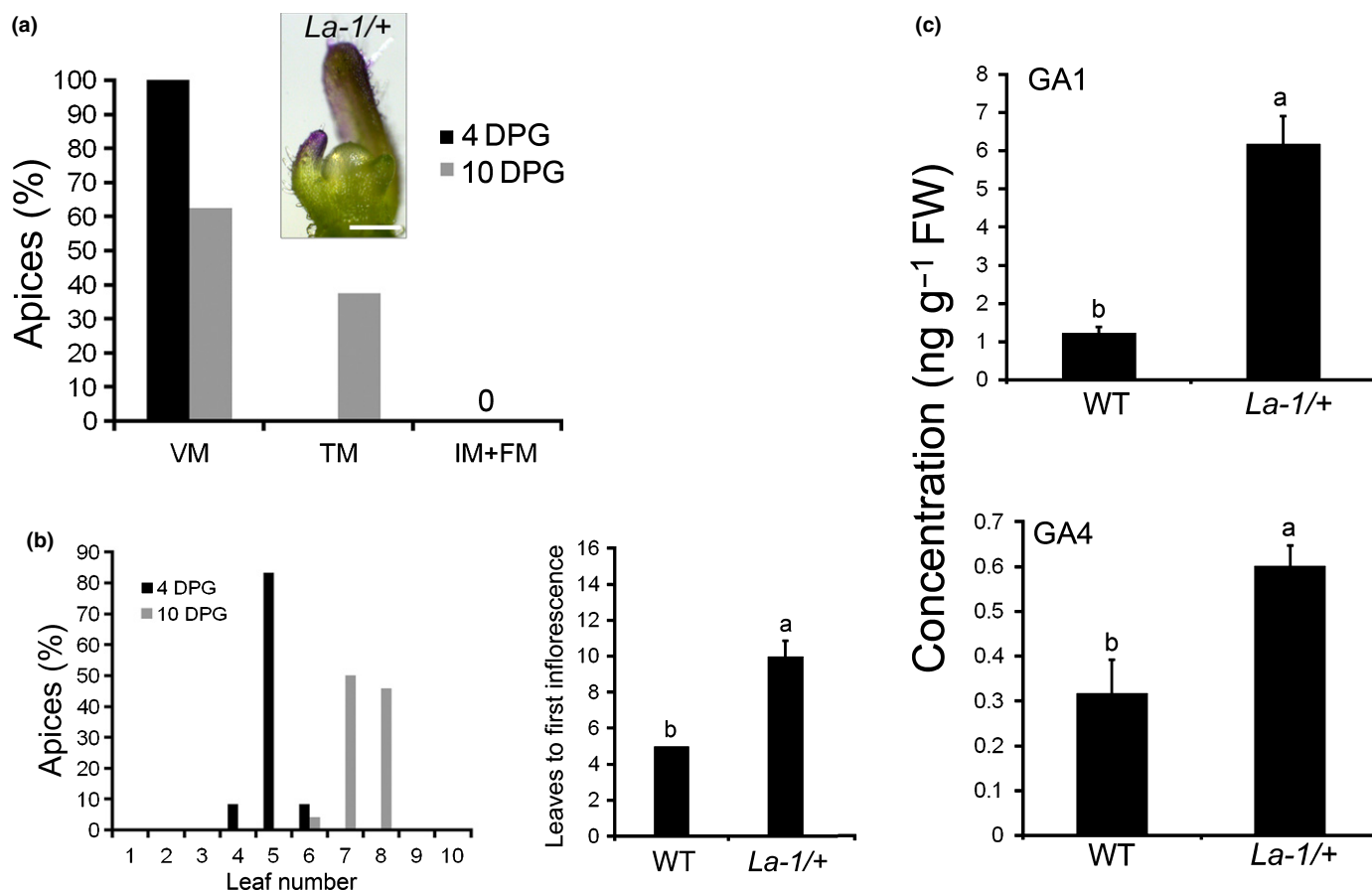


Fig. 5 Meristem maturation and flowering time are delayed in the *Lanceolate* mutant. (a) Meristem maturation (as depicted in Fig. 1) was evaluated in *La-1/+* mutant shoot apices ($n = 20$). Inset of a representative shoot apex at the vegetative meristem (VM) developmental stage is shown. Bar, 200 μ m. (b) Left: leaves generated by the primary shoot meristem counted from at least 20 *La-1/+* seedlings at each developmental stage (4, and 10 d post-germination, DPG). Right: flowering time in wild-type (WT) and *La-1/+* plants (mean \pm SD; $n = 12$). Distinct letters indicate significant difference according to Student's *t*-test ($P < 0.001$). (c) Bioactive gibberellin (GA) quantification (GA₁ and GA₄) in 4 DPG shoot apices of WT and *La-1/+*. Values are means \pm SD of three biological samples. Distinct letters indicate significant difference according to Student's *t*-test ($P < 0.01$).

(Fig. 2). The delay in floral transition in *La-1/+* shoot apices led to the production of six to eight leaf primordia at 10 DPG and *c.* 10 leaves in the primary shoot before flowering (Fig. 5b). Like previously described phenotypes (Stettler, 1964), *La-1/+* plants produced a lower number of flowers per inflorescence (Fig. S7b). Interestingly, *c.* 50% of *La-1/+* plants produced tendril-like structures in place of flowers (Fig. S7a). Together, these observations suggested that floral induction and inflorescence complexity are impaired in *La-1/+* mutant.

MiR319-targeted *LANCEOLATE* integrates with miR156-controlled and GA-associated pathways

Given that *LA* positively regulates *SlGA20ox1* expression (Yanai *et al.*, 2011), we hypothesized that *LA* modulates, directly or indirectly, endogenous GA concentrations during floral induction as well. We observed higher concentrations of both bioactive GA₁ and GA₄ in 4 DPG *La-1/+* apices (Fig. 5c), which agrees with the observed positive regulation of the GA concentrations by *LANCEOLATE*/TCP4 in tomato and *Arabidopsis* (Yanai *et al.*, 2011). Similar to GA₃-treated tomato and *GA20ox-OE* plants

(Fig. 4), high GA concentrations/responses may contribute to the delay in *La-1/+* meristem maturation and flower development (Fig. 5b).

The delay in *La-1/+* flowering transition (Fig. 5) resembled that from *pro* and 156-OE plants (Fig. 2), suggesting that *LANCEOLATE* may also intersect with *PRO/DELLA*-dependent GA responses and miR156-targeted *SlSBPs*. To test this hypothesis, we first measured *LA* transcript abundances in 4 and 10 DPG WT, *pro*, 156-OE, and *La-1/+* apices. At 4 DPG, *LA* was expressed at similar levels in all shoot apices, including *La-1/+*. However, higher *LA* transcript abundances were detected in 10 DPG apices from *pro* and *La-1/+* (Fig. 6a). These findings suggest that *LA* expression is regulated by *LANCEOLATE* and *PROCERA* at the reproductive stage, perhaps via miR319. This appears to be the case, as miR319 transcripts accumulated at lower levels in 10 DPG apices of *pro* and *La-1/+* plants (Fig. S8a).

To determine whether the delay in floral transition in *La-1/+* plants was caused by misregulation of *SlSBPs*, we measured *SlSBP3* and *SlSBP15* transcript abundances in shoot apices. *SlSBP3* and *SlSBP15* expression did not change in 4 DPG *La-1/+* apices (Figs 6b, S8b) and *SlSBP15* was similarly expressed in 10 DPG *La-*

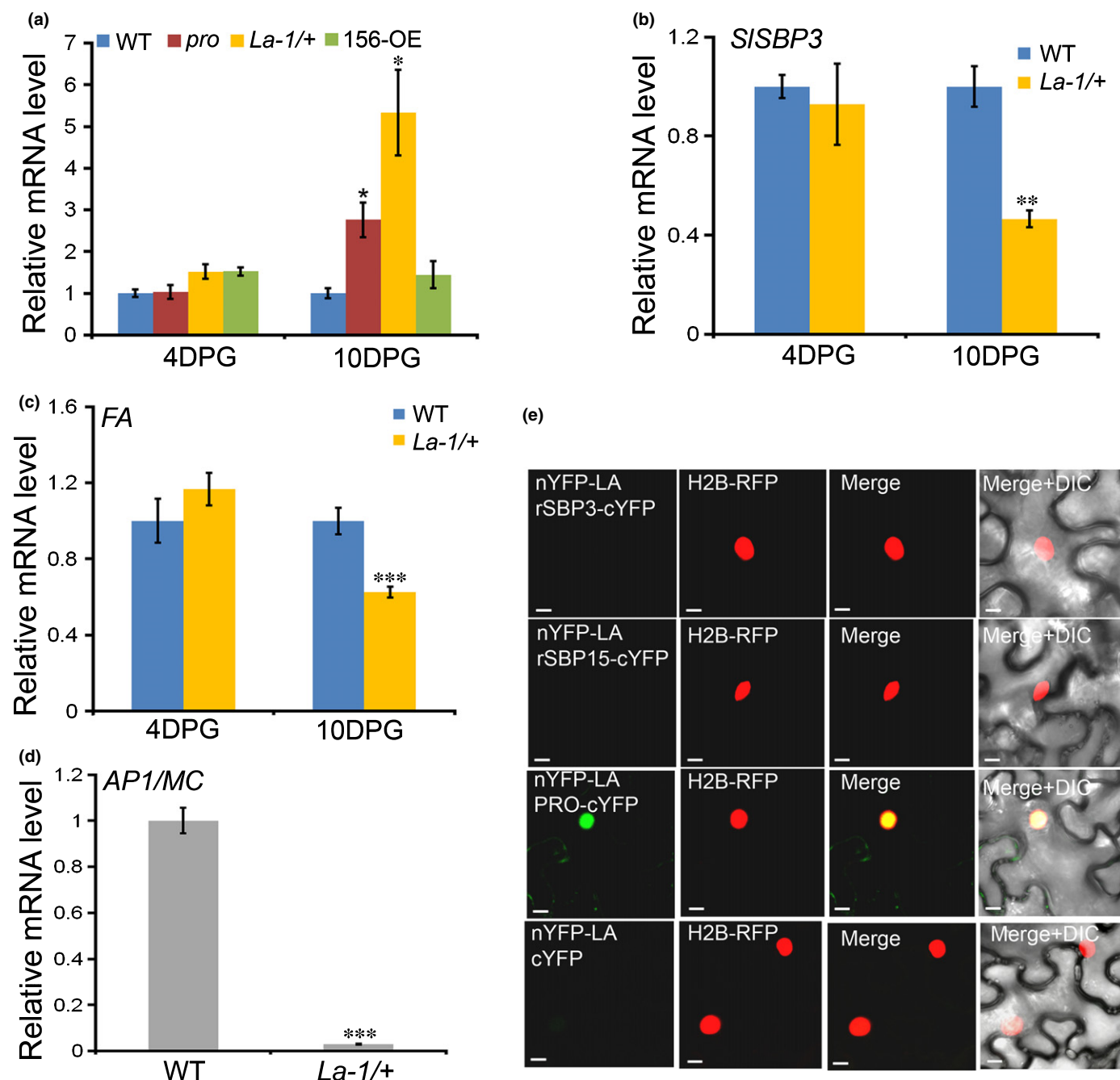


Fig. 6 MiR319-targeted *LANCEOLATE* (*LA*) represses the expression of key flowering identity genes. (a) *LA* expression levels in wild-type (WT), *pro*, *La-1/+*, and 156-OE shoot apices. These quantitative reverse transcription polymerase chain reaction (qRT-PCR) experiments used tissues from WT apices as the reference sample (set to 1.0). (b–d) Transcriptional levels of *SISBP3* (b), *FALSIFLORA* (*FA*) (c) and *APELATA1* (*AP1*)/*MC* (d) in WT and *La-1/+* shoot apices. Note that *AP1/MC* expression was only detected in 10 d post-germination (DPG) shoot apices (d). These qRT-PCR experiments used tissues from WT apices as the reference sample (set to 1.0). All qRT-qPCR values are means \pm SE of three biological samples. Tomato *TUBULIN* (Solyc04g081490) was used as an internal control. Asterisks indicate a significant difference when compared with reference sample according to Student's *t*-test (two tailed): *, $P < 0.05$; **, $P < 0.01$; ***, $P < 0.001$. (e) Bimolecular fluorescence complementation experiments using *Nicotiana benthamiana* leaves infiltrated with agrobacteria. The combination of nYFP-*LA* with cYFP was used as a negative control. Histone 2B (H2B)-RFP was used as a nuclear marker. The corresponding differential interference contrast (DIC) image combined with merged image (Merge + DIC) is also shown. The yellow color in the merged images indicates colocalization between coexpressed proteins. Bars, 10 μ m.

I/+ and WT apices (Fig. S8b). Nonetheless, *SISBP3* transcript abundances were reduced in 10 DPG *La-1/+* (Fig. 6b). *FA* expression did not change in *La-1/+* vegetative apices, but was down-regulated in 10 DPG *La-1/+* apices (Fig. 6c). *AP1/MC* transcripts

were barely detected in 10 DPG *La-1/+* apices, consistent with the delay in flower initiation (Fig. 6d). Thus, inflorescence development is delayed in *La-1/+* plants as a result of the repression of at least *SISBP3*, *FA*, and *AP1/MC* by *LANCEOLATE* at the SAM.

MiR156-targeted SPL9 (a SISBP15 homolog) binds directly to miR319-targeted TCP4 to modulate *Arabidopsis* leaf complexity, whereas class I TCPs form a complex with DELLAs to control plant height (Davière *et al.*, 2014; Rubio-Somoza *et al.*, 2014). Because our findings suggest that LANCEOLATE, miR156, and PRO/DELLA converge to regulate common floral identity genes (Figs 3, 6), we suspected that LA might bind directly to SISBPs and PROCERA/DELLA. We tested this hypothesis by performing Y2H and BiFC assays (Figs 6e, S5). While *SISBP3* did not show interaction with LA in either the Y2H or BiFC assays, *SISBP15* weakly interacted with LA in the Y2H assays (Fig. S5), an interaction that we could not confirm by BiFC assays (Fig. 6e). We concluded that LANCEOLATE does not interact directly with these two SISBPs. On the other hand, LANCEOLATE strongly interacts with PROCERA/DELLA (Figs 6e, S5). Such an interaction might be an additional mechanism by which GA partly mediates LANCEOLATE activity during tomato development (Yanai *et al.*, 2011).

To further investigate the functional relationship between LA and the age-controlled miR156/*SISBP* module during flowering, we tested for genetic interactions by introducing the *La-1* mutation into 156-OE plants, generating the 156-OE; *La-1/+* plants. Conspicuously, while 40-d-old WT and *La-1/+* plants already produced inflorescences and flowers, and all 40-d-old 156-OE plants displayed shoot apices at the IM + FM developmental stage, 40-d-old 156-OE; *La-1/+* apices did not produce any inflorescence. In fact, all 156-OE; *La-1/+* plants exhibited apices at the VM stage (Fig. 7a). Even after 100 DPG, 156-OE; *La-1/+* plants were not able to produce flowers, but instead some plants generated an undetermined structure from their apices, which did not show any reproductive identity (Fig. 7b). Few 156-OE; *La-1/+* plants produced structures that we referred as 'vegetative inflorescences' (Molinero-Rosales *et al.*, 1999) in place of the inflorescences (Fig. 7c). Together, our results show that LA and *SISBP*s act synergistically, but oppositely, to regulate floral transition and inflorescence identity.

To examine whether the unexpected nonflowering phenotype of 156-OE; *La-1/+* plants were reproducible in a nondwarf cultivar, we crossed hemizygous 156-OE plants with the original nondwarf *La* mutant (LA0335). We analyzed the vegetative and

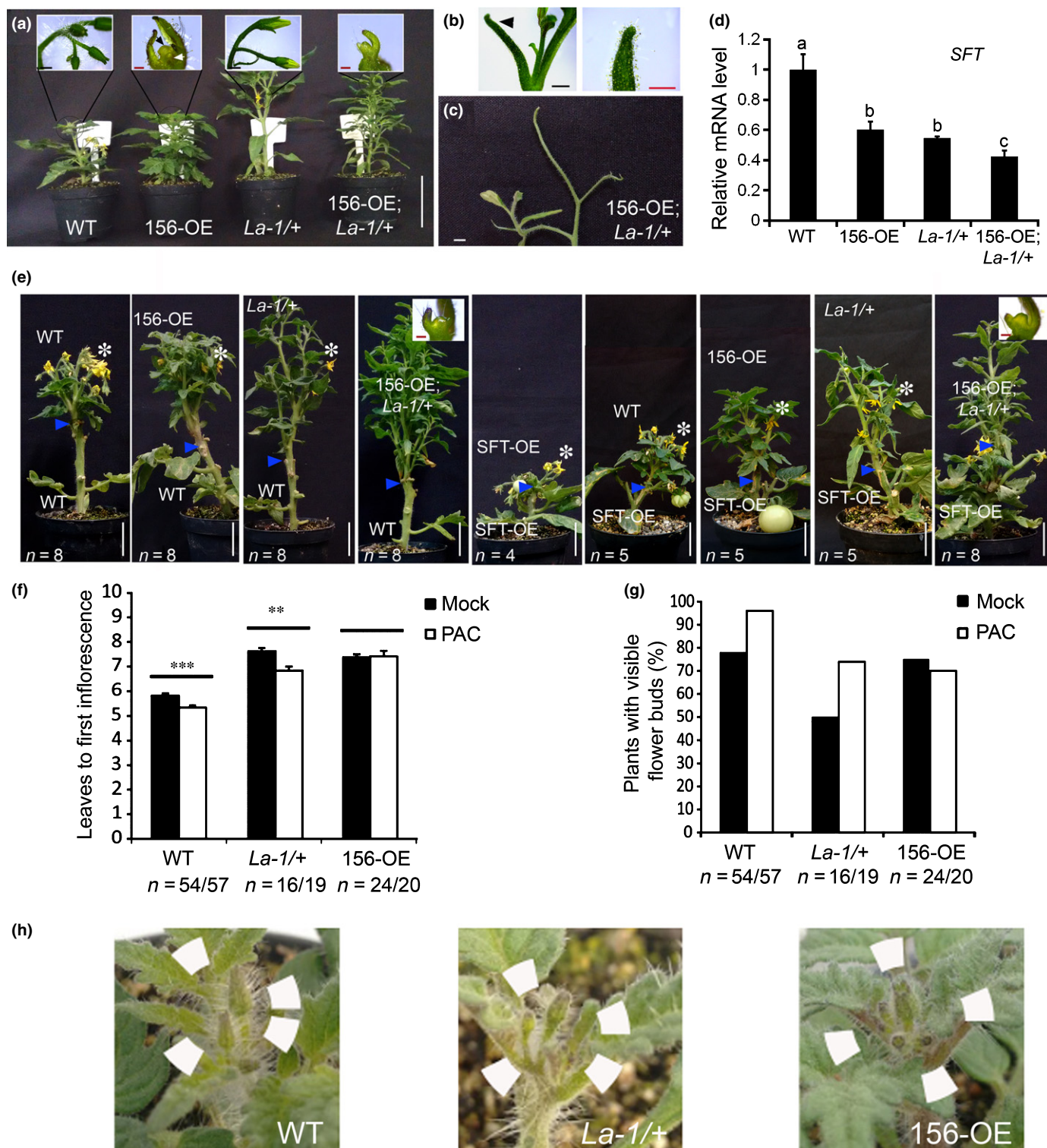
reproductive phenotypes of the F₁ offspring in which the recessive mutations of MT (Meissner *et al.*, 2000) are in the heterozygous form. The WT progeny from the cross produced normal vegetative and reproductive architectures, but those with the 35S: *AtMIR156b* transgene (Ferreira e Silva *et al.*, 2014) or the *La-1* mutation displayed a higher number of smaller leaves and late flowering (Fig. S9a,b), similar to 156-OE and *La-1/+* MT plants (Fig. 6a). Most importantly, 92% of the F₁ offspring 156-OE; *La-1/+* plants did not produce any apparent inflorescence (Fig. S9c), although 8.0% produced inflorescence-like structures (Fig. S9d). These observations indicated that LA and *SISBP*s act synergistically to control floral induction in the hybrid background as well. Although few 156-OE; *La-1/+* hybrids showed inflorescence-like structures (Fig. 9d), they produced a higher number of leaves to first inflorescence than did the *La-1/+* or 156-OE plants (Fig. S9b).

Given that floral transition was blocked in 156-OE; *La-1/+* (Figs 7a–c, S9), we suspected that not only were floral identity genes inactivated at the SAM (Fig. 6), but that *SFT* expression or *SFT*-derived signals were impaired in leaves. Indeed, *SFT* was down-regulated in leaf tissues of 156-OE and *La-1/+* plants, and further inhibited in 156-OE; *La-1/+* (Fig. 7d). We cannot rule out the possibility that floral induction was affected in 156-OE; *La-1/+* also as a result of modifications in general meristem activity. However, the stronger downregulation of *SFT* in 156-OE; *La-1/+* leaves (Fig. 7d) indicates that the transition to flowering is modulated by *SISBP*s and LA in both leaves and SAM. LA modulates tomato flowering time directly or indirectly through *SFT*, and this observation led us to hypothesize that an extra offer of graft-transmissible *SFT*-derived signals might trigger floral transition in 156-OE; *La-1/+* apices. *p35S::SFT* (SFT-OE) phenotypes in the MT background such as earlier flowering and shorter internodes were correlated with high *SFT* transcript abundances (Fig. S10), as previously described (Lifschitz *et al.*, 2006). Grafts using WT, 156-OE, and *La-1/+* as receptors (scions), and WT or SFT-OE as donors (rootstocks) were able to flower within 8 wk. By contrast, grafts involving WT or SFT-OE donors and 156-OE; *La-1/+* receptors failed to produce any inflorescence. Indeed, all grafted 156-OE; *La-1/+* displayed apices at the VM stage after 8 wk (Fig. 7e, insets). Even a persistent generation of systemic

Fig. 7 Interplay between miR319-targeted LANCEOLATE, miR156-targeted *SISBP*s, and gibberellin (GA) during floral transition and inflorescence development. (a) Representative *Solanum lycopersicum* wild-type (WT), 156-OE, *La-1/+*, and 156-OE; *La-1/+* plants. The insets show the apical shoot region of each genotype. Note that all 40-d-old 156-OE apices switched to the reproductive stage (the black arrow indicates floral meristem and the white arrow shows inflorescence meristem), whereas 100% of 40-d-old 156-OE; *La-1/+* apices were at the vegetative stage. (b) Representative apex of 100-d-old 156-OE; *La-1/+* plants. The right panel shows a magnification of the apex shown on the left panel (arrowhead). (c) Representative apex of a 100-d-old 156-OE; *La-1/+* plant showing the 'vegetative inflorescence' structure. (d) Transcriptional levels of *SINGLE FLOWER TRUSS* (*SFT*) in WT, 156-OE, *La-1/+*, and 156-OE; *La-1/+* leaves. These quantitative reverse transcription polymerase chain reaction (qRT-PCR) experiments used tissues from WT leaves as the reference sample (set to 1.0). qRT-PCR values are means \pm SE of three biological replicates. Tomato *TUBULIN* (Solyc04g081490) was used as an internal control. Distinct letters indicate significant difference according to Student's *t*-test ($P < 0.01$). (e) Graft-transmissible *SFT*-derived signals induce flowering in all scions (WT, 156-OE, and *La-1/+*), except for 156-OE; *La-1/+*. A donor (WT or SFT-OE) is grafted (blue arrowhead) below a receptor (WT, 156-OE, *La-1/+*, and 156-OE; *La-1/+*). Flowering response (asterisk) is followed in the released lateral shoots of the scion. The insets show the apical shoot region of the 156-OE; *La-1/+* scions. *n*, number of grafted plants. (f, g) WT, *La-1/+*, and 156-OE plants in the MT background were evaluated for the number of leaves to first inflorescence (f) and percentage of plants with visible floral buds (g). Plants were watered daily with paclobutrazol (PAC) and water (mock) during the first 20 d post-germination (DPG). The number of evaluated plants (*n*) is shown below of each genotype (mock/PAC). (h) Representative apices of 20 DPG plants treated with PAC. Floral buds are highlighted inside white circles. Values are means \pm SE. Asterisks indicate a significant difference when compared with reference sample (mock) according to Student's *t*-test: **, $P < 0.01$; ***, $P < 0.001$. Bars: (a) 8 cm (white), 2 mm (black), 50 μ m (red); (b) 2 mm (black), 50 μ m (red); (c) 2 mm; (e) 4 cm (white), 50 μ m (red).

SFT signal was not sufficient to promote floral transition in 156-OE; *La-1/+* plants, which suggested the meristem maturation was compromised in these plants. *FA* and *API1/MC* were already down-regulated in the shoot apices of 156-OE and *La-1/+* plants (Figs 3, 6), which may further impair *SFT*-mediated floral transition in 156-OE; *La-1/+* plants.

Unlike *La-1/+* plants (Figs 5, 7), *TCP4*-overexpressing *Arabidopsis* plants flower earlier than WT, partially by up-regulating the *SFT* homolog, *FT* (Kubota *et al.*, 2017; Liu *et al.*, 2017). The *Arabidopsis tcp4-soj8* mutant also flowers earlier as it contains a point mutation in the miRNA target site of *TCP4* that lessens the interaction with miR319, thus deregulating *TCP4*



(Palatnik *et al.*, 2007). We introduced *tcp4-soj8* mutation into *Arabidopsis* miR156-overexpressing plants (156-OE; Morea *et al.*, 2016) to determine whether *TCP4* deregulation might induce earlier flowering in 156-OE plants. Consistent with the role of *TCP4* in promoting flowering, both 30-d-old *tcp4-soj8/+* and 156-OE; *tcp4-soj8/+* plants produced visible flowers in LD conditions, whereas 30-d-old 156-OE plants were at the vegetative stage (Fig. S11). Although the *LANCEOLATE* homolog *TCP4* promotes photoperiodic flowering by activating *CONSTANS* (Liu *et al.*, 2017), it is currently unknown whether miR156-targeted *SPLs* or GA participate in this network as well.

Lower GA concentrations/responses trigger early flowering and inflorescence development in tomato

To investigate the direct effect of GA on tomato floral induction, we treated WT (MT), *La-1/+*, and 156-OE seedlings with PAC, an inhibitor of GA biosynthesis (Jung *et al.*, 2012). Tomato cv M82 seedlings were also subjected to similar PAC treatment to provide a broader understanding of the direct effects of GA on different tomato genetic backgrounds (Figs 7f–h, S12). After treatment for 20 DPG, differences in vegetative development and Chl content were observed between mock-treated and PAC-treated plants, which support the efficiency of PAC treatment (Pal *et al.*, 2016). As expected, PAC-treated plants had reduced plant height and higher Chl content in leaves (Figs S12, S13), suggesting a conservative effect of GA on tomato vegetative development. Most importantly, we assessed the effect of low GA responses or high levels of PROCERA/DELLA (via PAC treatment) on tomato floral induction. Notably, the PAC-treated WT (MT) produced a significantly lower number of leaves to first inflorescence, indicating that tomato floral transition was promoted by low GA concentrations/responses (Fig. 7f). Transition to flowering was also promoted in PAC-treated M82 plants (Fig. S12a), similar to plants overexpressing constitutively active stable PROCERA protein (Fig. S2). Flower initiation was also promoted by reduced GA concentrations/responses, as, after 20 DPG of PAC treatment, almost 100% of WT (MT) plants displayed visible buds, compared with <80% of mock-treated MT plants (Fig. 7g,h). Remarkably, <10% of mock-treated M82 plants displayed visible buds after 20 DPG. Conversely, 60% of PAC-treated M82 plants displayed noticeable buds in the same period (Fig. S12b), indicating that GA concentrations/responses strongly affect inflorescence development in M82 plants. These observations support the direct effect of GA on transition to flowering and inflorescence development in tomato.

Floral transition and flower initiation were both promoted in PAC-treated *La-1/+* plants (Fig. 7f–h). However, PAC treatment did not restore WT phenotype in *La-1/+* plants in terms of floral induction (Fig. 7f,g). PAC-treated WT plants flowered after producing five leaves, whereas PAC-treated *La-1/+* flowered after seven leaves (Fig. 7f). The fact that *La-1/+* plants flowered earlier after PAC treatment indicates that GA responses partly mediate *LANCEOLATE* activity on floral induction. A similar response is observed during tomato leaf development, in which the miR319 overexpression phenotype is suppressed by GA

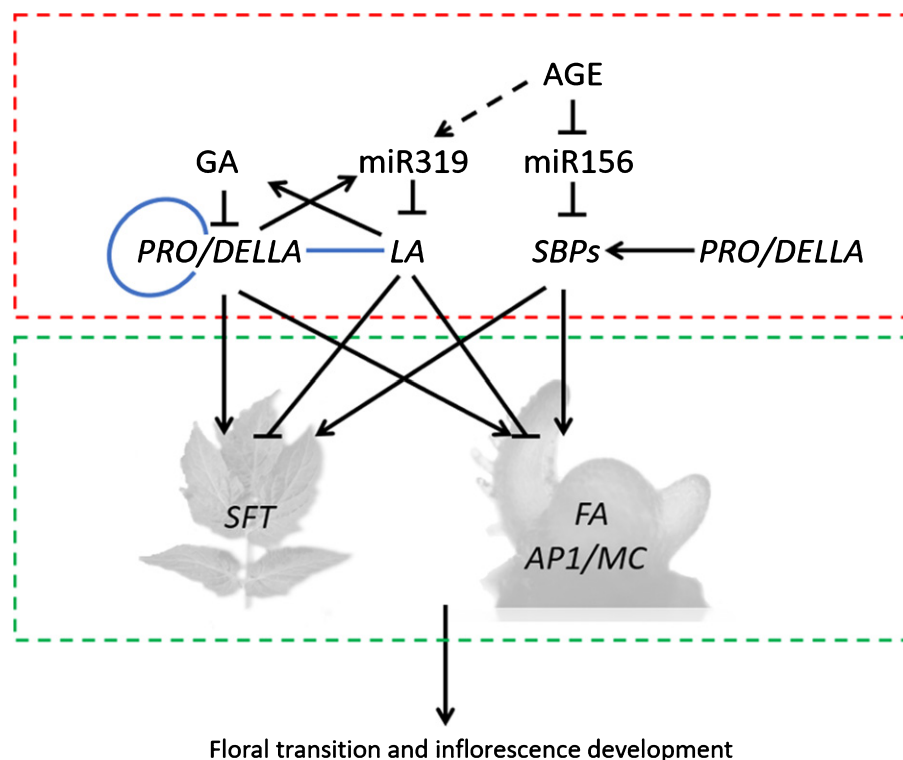
application and *pro* mutation (Yanai *et al.*, 2011). Although PAC-treated 156-OE plants presented similar modifications to WT and *La-1/+* in terms of Chl content, plant height differences between mock- and PAC-treated 156-OE plants were less pronounced (Fig. S13a,b). Most importantly, 156-OE plants were insensitive to PAC treatment in terms of floral transition and floral initiation (Fig. 7f,g). These observations suggest that a high level of PROCERA/DELLA (or low GA response) promotes tomato floral induction through miR156-targeted *SISBP*s (Fig. 2g; Yu *et al.*, 2012).

Discussion

Understanding how the flowering pathways integrate is of great importance to reveal how plants flower in response to developmental and environmental signals. Domesticated tomato is insensitive to at least two (namely, photoperiod and vernalization) out of the five flowering pathways described in the facultative LD *Arabidopsis* (Lozano *et al.*, 2009), but tomato floral induction is regulated by age and GA-associated pathways. The interplay between GA and miR156-*SISBP*s and miR319-*LA* modules during tomato floral induction is summarized in Fig. 8. We show here that reduced *PRO/DELLA* activity or increasing GA responses delay meristem maturation and flowering time in tomato, whereas low GA responses promote it. In *Fuchsia*, GA delays flowering time by blocking the florigenic effect of sucrose (King & Ben-Tal, 2001). It is possible that high GA responses may reduce sucrose import into the tomato SAM, which is a stimulus to flowering in several species (Bolouri-Moghaddam & Van den Ende, 2013). *Pisum sativum* plants overexpressing *PsGA3ox1* (which catalyzes the conversion of GA₂₀ to bioactive GA₁) display delayed flowering (Reinecke *et al.*, 2013), similarly to tomato *pro* and *GA20ox-OE* plants (Figs 2–4). These data suggest that the inhibitory effect of GA on flowering transition is not unique to tomato, but rather is shared with other species.

MiR156 and *SPL/SBP*s are regulated by aging and, as expected, miR156 overexpression in tomato leads to late-flowering phenotype, similar to *Arabidopsis* (Fig. 2; Yu *et al.*, 2012). However, unlike *Arabidopsis*, age-regulated miR156 acts cooperatively with GAs to delay tomato flowering time. We showed that *PRO/DELLA* and miR156-targeted *SISBP*s are required to promote tomato flowering in the leaves by activating *SFT* expression and therefore inducing *SFT*-derived signals; and at the SAM by activating floral identity genes as *FA* and *API/MC* (Figs 3, S3). *Arabidopsis* DELLAs delay floral transition by interfering with the transcription abundances and transcriptional activities of *SBP/SPL*s (Galvão *et al.*, 2012; Yu *et al.*, 2012; Hyun *et al.*, 2016). PROCERA/DELLA did not physically interact with *SISBP3* or *SISBP15* (Fig. 3), but rather regulates the transcriptional levels of these two *SISBP*s (and perhaps other *SISBP*s) at early stages of meristem maturation (Fig. 2). The relationship between DELLAs and *SBP/SPL* transcription factors differs depending on the developmental context (Yu *et al.*, 2012; Yamaguchi *et al.*, 2014; Hyun *et al.*, 2016). Therefore, it is possible that tomato *SBP*s not tested here are able to physically interact with *PRO/DELLA*. The fact that the transition to flowering was

Fig. 8 Hypothetical model for tomato floral transition and inflorescence development orchestrated by the crosstalk between gibberellins (GAs) and two unrelated miRNA modules. PRO/DELLA – a repressor of GA (GA) responses – promotes, directly or indirectly, *SINGLE FLOWER TRUSS* (*SFT*) expression in leaves and miR156-targeted *SBPs* and *APETALA1* (*AP1*)/*MC* at the shoot apex. PRO/DELLA interacts with itself as well as physically binding to *LANCEOLATE* (*LA*), perhaps to inhibit *LA* transcriptional repression towards flowering genes. *LA* is repressed by miR319 and positively controls GA concentrations. By interplaying with PRO/DELLA, miR156 and miR319 modules probably adjust GA responses to orchestrate transition to flowering in tomato. Blue lines represent protein–protein interactions. Arrows, promotion effects (directly or indirectly); T-bars, repression effects (directly or indirectly); dashed arrow, unclear interaction. Red dashed lines, floral promoters/repressors; green dashed lines, floral effectors.



further delayed in GA₃-treated 156-OE and 156-OE; *pro* plants (Figs 3, 4) suggests that PRO/DELLA also acts in parallel with *SISBP*s to regulate flowering genes. It is possible that by repressing several *SISBP*s (Ferreira e Silva *et al.*, 2014) miR156-overexpressing tomato plants alter their responsiveness to GA. This hypothesis is supported by the observation that miR156-overexpressing tomato plants did not respond to PAC treatment in terms of floral induction (Fig. 7), which is comparable to miR156-overexpressing *Arabidopsis* plants (Yu *et al.*, 2012).

Like tomato, rice has only one DELLA (SLENDER RICE1), which forms a homodimer essential for signal perception and repression activity (Itoh *et al.*, 2002). Our results indicate that PROCERA/DELLA binds to itself (Fig. 3), which might be pivotal for its repression activity. Mutation in the VHIID domain of PROCERA/DELLA in the *pro* mutant (Bassel *et al.*, 2008) may have impaired its ability to form homodimers and presumably heterodimers with transcription factors. One of these transcription factors is LANCEOLATE, as PRO/DELLA physically binds to LA (Fig. 6). Reduced activity of PRO/DELLA in *pro* plants or excess of LA protein in *La-1/+* plants may alter the proper function of the PRO/DELLA–LA complex. The direct interaction between PRO/DELLA and LA suggests a molecular link, but further investigation is necessary to uncover the mechanisms by which PRO/DELLA and LA may regulate common targets. One possibility is that PRO/DELLA attenuates LA transcriptional repression toward its targets, a mechanism for which has been shown for the interaction between *Arabidopsis* DELLAs and class I TCPs (Davière *et al.*, 2014). Meanwhile, PRO/DELLA interacts with the miR319–LA module at transcriptional levels. LA transcripts accumulated at higher levels, whereas

miR319 transcript abundances were lower in *pro* apices (Figs 6, S8). Together, these observations suggest a complex interplay between PROCERA/DELLA and the miR319–LANCEOLATE module during floral induction.

The role of tomato class II TCPs in flowering time was proposed in a previous study (Burko *et al.*, 2013). Unlike its homolog (*TCP4*) in *Arabidopsis*, we show that LANCEOLATE and *SISBP*s have opposing roles in regulating floral transition in tomato. While *SISBP*s promote flowering, LA suppresses it by down-regulating key flowering genes, and perhaps, by increasing GA concentrations/responses at the SAM (Figs 5–7). Remarkably, the combination of high levels of LA/TCP4 with low *SBP*/SPL levels led to opposing flowering phenotypes in tomato and *Arabidopsis*. While floral induction was promoted in 156-OE; *tcp4-soj8/+*, it was completely suppressed in 156-OE; *La-1/+* plants (Figs 7, S11). MiR319-targeted *TCP4/LA* and miR156-regulated *SPL/SBP*s probably control meristem maturation through common targets, but at this point it is unknown what mechanisms underlie the distinct relationships between these miRNA modules in *Arabidopsis* and tomato. One possibility is that *TCP4* and LA may have acquired specific targets in distinct species. In *Arabidopsis* leaves, miR156-targeted *SPL*s act in parallel with photoperiod-responsive *CONSTANS*, both of which are positive regulators of *FT*. *CONSTANS* is also the main target of *TCP4* during *Arabidopsis* floral transition (Sarvepalli & Nath, 2011; Kubota *et al.*, 2017; Liu *et al.*, 2017). Domesticated tomato is considered to be insensitive or less responsive to photoperiodic stimulus (Lozano *et al.*, 2009), and thus it is unlikely that tomato *CONSTANS* is a target of LANCEOLATE or acts in parallel with *SISBP*s. This idea is further supported by earlier

observations that overexpression of tomato or *Arabidopsis* *CONSTANS* does not affect tomato flowering time (Ben-Naim *et al.*, 2006). We propose that *LANCEOLATE* modulates tomato nonphotoperiodic flowering by inactivating floral integrators, including *SFT* and *API/MC*.

The synergistic and additive effects observed in our double mutants (Figs 3, 7) suggest that age (miR156-targeted *SISBP3*), *PROCERA/DELLA*, and miR319-targeted *LANCEOLATE* are integrated but their functions do not completely overlap during floral transition. This indicates that additional interactions and flowering targets for these pathways must exist. In fact, even the floral integrators regulated by age and GA-associated pathways (i.e. *SFT* and *API/MC*) seem to have complex and additional interactions. Despite being misregulated in the *fft* mutant, genetic analyses of double and single mutants show that *API/MC* synergistically interacts with *SFT* to control floral induction and inflorescence development (Yuste-Lisbona *et al.*, 2016). It is tempting to speculate that the domestication process of tomato may have eliminated redundancy in flowering genes, altering how GAs and microRNA targets interact with each other. It will be interesting to see how the age pathway is integrated with GA-associated pathways during meristem maturation and floral induction in wild tomato relatives.








Acknowledgements

We thank Dr C. Schommer for kindly providing *tcp4-soj8/+* seeds, and Carlos Rojas for *Arabidopsis* flowering time analyses. This work was supported by FAPESP (grant no. 15/17892-7 and fellowships nos 15/23826-7 and 13/16949-0). The authors declare no conflict of interest.

Author contributions

GFFS, EMS and FTSN planned and designed the research; GFFS, EMS, NJ, MHV, MMN, ACJ, JPOC, FAJ, and PC performed research; EC, IL-D, EG and LEPP contributed new reagents/analytic tools and genetic material; GFFS, EMS, NJ, MHV and FTSN analyzed data; and GFFS and FTSN wrote the paper.

ORCID

Joao P. O. Correa  <http://orcid.org/0000-0003-0692-7416>
 Erich Grotewold  <http://orcid.org/0000-0002-4720-7290>
 Nan Jiang  <http://orcid.org/0000-0002-9696-5784>
 Isabel López-Díaz  <http://orcid.org/0000-0003-4000-1633>
 Fabio T. S. Nogueira  <http://orcid.org/0000-0001-6613-4069>
 Lazaro E. P. Peres  <http://orcid.org/0000-0002-8761-5934>
 Mateus H. Vicente  <http://orcid.org/0000-0003-4885-8404>

References

- Andrés F, Coupland G. 2012. The genetic basis of flowering responses to seasonal cues. *Nature Review Genetics* 13: 627–639.
- Bassel GW, Mullen RT, Bewley JD. 2008. *Procera* is a putative DELLA mutant in tomato (*Solanum lycopersicum*): effects on the seed and vegetative plant. *Journal of Experimental Botany* 59: 585–593.
- Ben-Naim O, Eshed R, Parnis A, Teper-Bamnolker P, Shalit A, Coupland G, Samach A, Lifschitz E. 2006. The CCAAT binding factor can mediate interactions between *CONSTANS*-like proteins and DNA. *Plant Journal* 46: 462–476.
- Bolouri-Moghaddam MR, Van den Ende W. 2013. Sugars, the clock and transition to flowering. *Frontiers Plant Science* 4: 22.
- Boss PK, Thomas MR. 2002. Association of dwarfism and floral induction with a grape 'green revolution' mutation. *Nature* 416: 847–850.
- Burko Y, Shleizer-Burko S, Yanai O, Schwartz I, Zelnik ID, Jacob-Hirsch J, Kela I, Eshed-Williams L, Ori N. 2013. A role for APETALA1/fruitfull transcription factors in tomato leaf development. *Plant Cell* 25: 2070–2083.
- Cardon G, Höhmann S, Klein J, Nettessheim K, Saedler H, Huijser P. 1999. Molecular characterisation of the *Arabidopsis* *SBP-box* genes. *Gene* 237: 91–104.
- Carrera E, Ruiz-Rivero O, Peres LE, Amares A, Garcia-Martinez JL. 2012. Characterization of the *procera* tomato mutant shows novel functions of the *SIDE* protein in the control of flower morphology, cell division and expansion, and the auxin-signaling pathway during fruit-set and development. *Plant Physiology* 160: 1581–1596.
- Carvalho RF, Campos ML, Pino LE, Crestana SL, Zsögön A, Lima JE, Benedito VA, Peres LE. 2011. Convergence of developmental mutants into a single tomato model system: 'Micro-Tom' as an effective toolkit for plant development research. *Plant Methods* 7: 18.
- Cubas P, Lauter N, Doebley J, Coen E. 1999. The TCP domain: a motif found in proteins regulating plant growth and development. *Plant Journal* 18: 215–222.
- Davière JM, Wild M, Regnault T, Baumberger N, Eisler H, Genschik P, Achard P. 2014. Class I TCP-DELLA interactions in inflorescence shoot apex determine plant height. *Current Biology* 24: 1923–1928.
- Ferreira e Silva GF, Silva EM, Azevedo M da S, Guivin MA, Ramiro DA, Figueiredo CR, Carrer H, Peres LE, Nogueira FTS. 2014. microRNA156-targeted SPL/SBP box transcription factors regulate tomato ovary and fruit development. *Plant Journal* 78: 604–618.
- Gallego-Bartolomé J, Minguet EG, Marín JA, Prat S, Blázquez MA, Alabadí D. 2010. Transcriptional diversification and functional conservation between DELLA proteins in *Arabidopsis*. *Molecular Biology Evolution* 27: 1247–1256.
- Gallego-Giraldo L, García-Martínez JL, Moritz T, López-Díaz I. 2007. Flowering in tobacco needs gibberellins but is not promoted by the levels of active GA1 and GA4 in the apical shoot. *Plant Cell Physiology* 48: 615–625.
- Galvão VC, Horrer D, Küttner F, Schmid M. 2012. Spatial control of flowering by DELLA proteins in *Arabidopsis thaliana*. *Development* 139: 4072–4082.
- García-Hurtado N, Carrera E, Ruiz-Rivero O, López-Gresa MP, Hedden P, Gong F, García-Martínez JL. 2012. The characterization of transgenic tomato overexpressing gibberellin 20-oxidase reveals induction of parthenocarpic fruit growth, higher yield, and alteration of the gibberellin biosynthetic pathway. *Journal of Experimental Botany* 63: 5803–5813.
- Gargul JM, Mibus H, Serek M. 2013. Constitutive overexpression of *Nicotiana* *GA2ox* leads to compact phenotypes and delayed flowering in *Kalanchoe blossfeldiana* and *Petunia hybrida*. *Plant Cell, Tissue and Organ Culture* 115: 407–418.
- Goldberg-Moeller R, Shalom L, Shlizerman L, Samuels S, Zur N, Ophir R, Blumwald E, Sadka A. 2013. Effects of gibberellin treatment during flowering induction period on global gene expression and the transcription of flowering-control genes in *Citrus* buds. *Plant Science* 198: 46–57.
- Hauvermale AL, Ariizumi T, Steber CM. 2012. Gibberellin signaling: a theme and variations on DELLA repression. *Plant Physiology* 160: 83–92.
- Hyun Y, Richter R, Vincent C, Martinez-Gallegos R, Porri A, Coupland G. 2016. Multi-layered regulation of *SPL15* and cooperation with *SOC1* integrate endogenous flowering pathways at the *Arabidopsis* shoot meristem. *Developmental Cell* 37: 254–266.
- Itoh H, Ueguchi-Tanaka M, Sato Y, Ashikari M, Matsuoka M. 2002. The gibberellin signaling pathway is regulated by the appearance and disappearance of SLENDER RICE1 in nuclei. *Plant Cell* 14: 57–70.

- James P, Halladay J, Craig EA. 1996. Genomic libraries and a host strain designed for highly efficient two-hybrid selection in yeast. *Genetics* 144: 1425–1436.
- Jung JH, Ju Y, Seo PJ, Lee JH, Park CM. 2012. The SOC1-SPL module integrates photoperiod and gibberellin acid signals to control flowering time in *Arabidopsis*. *Plant Journal* 69: 577–588.
- King RW, Ben-Tal Y. 2001. A florigenic effect of sucrose in *Fuchsia hybrida* is blocked by gibberellin-induced assimilate competition. *Plant Physiology* 125: 488–496.
- Kubota A, Ito S, Shim JS, Johnson RS, Song YH, Breton G, Goraloglia GS, Kwon MS, Laboy Cintrón D, Koyama T *et al.* 2017. TCP4-dependent induction of *CONSTANS* transcription requires *GIGANTEA* in photoperiodic flowering in *Arabidopsis*. *PLoS Genetics* 13: e1006856.
- Kudla J, Bock R. 2016. Lighting the way to protein-protein interactions: recommendations on best practices for bimolecular fluorescence complementation (BiFC) analyses. *Plant Cell* 28: 1002–1008.
- Lifschitz E, Eviatar T, Rozman A, Shalit A, Goldshmidt A, Amsellem Z, Alvarez JP, Eshed Y. 2006. The tomato FT ortholog triggers systemic signals that regulate growth and flowering and substitute for diverse environmental stimuli. *Proceedings of the National Academy of Sciences, USA* 103: 6398–6403.
- Liu J, Cheng X, Liu P, Li D, Chen T, Gu X, Sun J. 2017. MicroRNA319-regulated TCPs interact with FBHs and PFT1 to activate CO transcription and control flowering time in *Arabidopsis*. *PLoS Genetics* 13: e1006833.
- Livak KJ, Schmittgen TD. 2001. Analysis of relative gene expression data using real-time quantitative PCR and the 2DDCT method. *Methods* 25: 402–408.
- Livne S, Lor VS, Nir I, Eliaz N, Aharoni A, Olszewski NE, Eshed Y, Weiss D. 2015. Uncovering DELLA-independent gibberellin responses by characterizing new tomato *procera* mutants. *Plant Cell* 27: 1579–1594.
- Lombardi-Crestana S, da Silva Azevedo M, e Silva GF, Pino LE, Appezzato-da-Glória B, Figueira A, Nogueira FT, Peres LE. 2012. The tomato (*Solanum lycopersicum* cv. Micro-Tom) natural genetic variation *Rgl* and the DELLA mutant *procera* control the competence necessary to form adventitious roots and shoots. *Journal of Experimental Botany* 63: 5689–5703.
- Lozano R, Giménez E, Cara B, Capel J, Angosto T. 2009. Genetic analysis of reproductive development in tomato. *International Journal of Developmental Biology* 53: 1635–1648.
- Martin K, Kopperud K, Chakrabarty R, Banerjee R, Brooks R, Goodin MM. 2009. Transient expression in *Nicotiana benthamiana* fluorescent marker lines provides enhanced definition of protein localization, movement and interactions in *planta*. *Plant Journal* 59: 150–162.
- Martínez-bello L, Moritz T, López-díaz I. 2015. Silencing *C19-GA 2-oxidases* induces parthenocarpic development and inhibits lateral branching in tomato plants. *Journal of Experimental Botany* 66: 5897–5910.
- Meissner R, Chague V, Zhu Q, Emmanuel E, Elkind Y, Levy AA. 2000. Technical advance: a high throughput system for transposon tagging and promoter trapping in tomato. *Plant Journal* 22: 265–274.
- Molinero-Rosales N, Jamilena M, Zurita S, Gómez P, Capel J, Lozano R. 1999. *FALSIFLORA*, the tomato orthologue of *FLORICAULA* and *LEAFY*, controls flowering time and floral meristem identity. *Plant Journal* 20: 685–693.
- Morea EG, da Silva EM, Silva GF, Valente GT, Barrera Rojas CH, Vincentz M, Nogueira FT. 2016. Functional and evolutionary analyses of the miR156 and miR529 families in land plants. *BMC Plant Biology* 16: 40.
- Mounet F, Moing A, García V, Petit J, Maucourt M, Deborde C, Bernillon S, Le Gall G, Colquhoun I, Defernez M *et al.* 2009. Gene and metabolite regulatory network analysis of early developing fruit tissues highlight new candidate genes for the control of tomato fruit composition and development. *Plant Physiology* 149: 1505–1528.
- Nir I, Shohat H, Panizel I, Olszewski N, Aharoni A, Weiss D. 2017. The tomato DELLA protein PROCERA acts in guard cells to promote stomatal closure. *Plant Cell* 29: 3186–3197.
- Ohad N, Shichrur K, Yalovsky S. 2007. The analysis of protein-protein interactions in plants by bimolecular fluorescence complementation. *Plant Physiology* 145: 1090–1099.
- Ori N, Cohen AR, Etzioni A, Brand A, Yanai O, Shleizer S, Menda N, Amsellem Z, Efroni I, Pekker I, *et al.* 2007. Regulation of *LANCEOLATE* by miR319 is required for compound-leaf development in tomato. *Nature Genetics* 39: 787–791.
- Pal S, Zhao J, Khan A, Yadav NS, Batushansky A, Barak S, Rewald B, Fait A, Lazarovitch N, Rachmilevitch S. 2016. Paclobutrazol induces tolerance in tomato to deficit irrigation through diversified effects on plant morphology, physiology and metabolism. *Scientific Reports* 6: 39321.
- Palatnik JF, Wollmann H, Schommer C, Schwab R, Boissbouvier J, Rodriguez R, Warthmann N, Allen E, Dezulian T, Huson D *et al.* 2007. Sequence and expression differences underlie functional specialization of Arabidopsis microRNAs miR159 and miR319. *Developmental Cell* 13: 115–125.
- Parapunova V, Busscher M, Busscher-Lange J, Lammers M, Karlova R, Bovy AG, Angenent GC, de Maagd RA. 2014. Identification, cloning and characterization of the tomato TCP transcription factor family. *BMC Plant Biology* 14: 157.
- Park SJ, Jiang K, Schatz MC, Lippman ZB. 2012. Rate of meristem maturation determines inflorescence architecture in tomato. *Proceedings of the National Academy of Sciences, USA* 109: 639–644.
- Pharis R, King R. 1985. Gibberellins and reproductive development in seed plants. *Annual Review of Plant Physiology* 36: 517–568.
- Porri A, Torti S, Romera-Branchat M, Coupland G. 2012. Spatially distinct regulatory roles for gibberellins in the promotion of flowering of *Arabidopsis* under long photoperiods. *Development* 139: 2198–2209.
- Preston JC, Hileman LC. 2013. Functional evolution in the plant SQUAMOSA-PROMOTER BINDING PROTEIN-LIKE (SPL) gene family. *Frontiers Plant Science* 4: 80.
- Quinet M, Kinet J-M. 2007. Transition to flowering and morphogenesis of reproductive structures in tomato. *International Journal of Plant Development Biology* 1: 64–74.
- Reinecke DM, Wickramarathna AD, Ozga JA, Kurepin LV, Jin AL, Good AG, Pharis RP. 2013. Gibberellin 3-oxidase gene expression patterns influence gibberellin biosynthesis, growth, and development in pea. *Plant Physiology* 163: 929–945.
- Rubio-Somoza I, Weigel D. 2011. MicroRNA networks and developmental plasticity in plants. *Trends Plant Science* 16: 258–264.
- Rubio-Somoza I, Zhou CM, Confraria A, Martinho C, von Born P, Baena-Gonzalez E, Wang JW, Weigel D. 2014. Temporal control of leaf complexity by miRNA-regulated licensing of protein complexes. *Current Biology* 24: 2714–2719.
- Salinas M, Xing S, Höhmans S, Berndtgen R, Huijser P. 2012. Genomic organization, phylogenetic comparison and differential expression of the SBP-box family of transcription factors in tomato. *Planta* 235: 1171–1184.
- Sarvepalli K, Nath U. 2011. Hyper-activation of the TCP4 transcription factor in *Arabidopsis thaliana* accelerates multiple aspects of plant maturation. *Plant Journal* 67: 595–607.
- Serrano-Mislata A, Bencivenga S, Bush M, Schiessl K, Boden S, Sablowski R. 2017. *DELLA* genes restrict inflorescence meristem function independently of plant height. *Nature Plants* 9: 749–754.
- Shikata M, Ezura H. 2016. Micro-Tom Tomato as an alternative plant model system: mutant collection and efficient transformation. *Methods in Molecular Biology* 1363: 47–55.
- Stettler RF. 1964. Dosage effects of the *Lanceolate* gene in tomato. *American Journal of Botany* 51: 253–264.
- Varkonyi-Gasic E, Wu R, Wood M, Walton EF, Hellens RP. 2007. Protocol: a highly sensitive RT-PCR method for detection and quantification of microRNAs. *Plant Methods* 3: 12.
- Vendemiatti E, Zsögön A, Silva GF, de Jesus FA, Cutri L, Figueiredo CRF, Tanaka FAO, Nogueira FTS, Peres LEP. 2017. Loss of type-IV glandular trichomes is a heterochronic trait in tomato and can be reverted by promoting juvenility. *Plant Science* 259: 35–47.
- Vicente MH, Zsögön A, de Sá AFL, Ribeiro RV, Peres LEP. 2015. Semi-determinate growth habit adjusts the vegetative-to-reproductive balance and increases productivity and water-use efficiency in tomato (*Solanum lycopersicum*). *Journal Plant Physiology* 177: 11–19.
- Wang JW, Czech B, Weigel D. 2009. miR156-regulated SPL transcription factors define an endogenous flowering pathway in *Arabidopsis thaliana*. *Cell* 138: 738–749.
- Wilkie JD, Sedgley M, Olesen T. 2008. Regulation of floral initiation in horticultural trees. *Journal of Experimental Botany* 59: 3215–3228.

- Yamaguchi A, Wu MF, Yang L, Wu G, Poethig RS, Wagner D. 2009. The microRNA-regulated SBP-Box transcription factor SPL3 is a direct upstream activator of *LEAFY*, *FRUITFULL*, and *APETALA1*. *Developmental Cell* 17: 268–278.
- Yamaguchi N, Winter CM, Wu MF, Kanno Y, Yamaguchi A, Seo M, Wagner D. 2014. Gibberellin acts positively then negatively to control onset of flower formation in *Arabidopsis*. *Science* 344: 638–641.
- Yamaguchi S. 2008. Gibberellin metabolism and its regulation. *Annual Review of Plant Biology* 59: 225–251.
- Yamamoto A, Nakamura T, Adu-Gyamfi JJ, Saigusa M. 2002. Relationship between chlorophyll content in leaves of sorghum and pigeonpea determined by extraction method and by chlorophyll meter (SPAD-502). *Journal of Plant Nutrition* 25: 2295–2301.
- Yanai O, Shani E, Russ D, Ori N. 2011. Gibberellin partly mediates *LANCEOLATE* activity in tomato. *Plant Journal* 68: 571–582.
- Yu S, Galvão VC, Zhang YC, Horrer D, Zhang TQ, Hao YH, Feng YQ, Wang S, Schmid M, Wang JW. 2012. Gibberellin regulates the *Arabidopsis* floral transition through miR156-targeted *SQUAMOSA* promoter binding-like transcription factors. *Plant Cell* 24: 3320–3332.
- Yuste-Lisbona FJ, Quinet M, Fernández-Lozano A, Pineda B, Moreno V, Angosto T, Lozano R. 2016. Characterization of vegetative inflorescence (*mc-vin*) mutant provides new insight into the role of *MACROCALYX* in regulating inflorescence development of tomato. *Scientific Reports* 6: 18796.
- Zhang S, Zhang D, Fan S, Du L, Shen Y, Xing L, Li Y, Ma J, Han M. 2016. Effect of exogenous GA₃ and its inhibitor paclobutrazol on floral formation, endogenous hormones, and flowering-associated genes in ‘Fuji’ apple (*Malus domestica* Borkh.). *Plant Physiology Biochemistry* 107: 178–186.
- Zhang X, Zou Z, Zhang J, Zhang Y, Han Q, Hu T, Xu X, Liu H, Li H, Ye Z. 2011. Over-expression of *sly-miR156a* in tomato results in multiple vegetative and reproductive trait alterations and partial phenocopy of the *sfi* mutant. *Febs Letters* 585: 435–439.

Supporting Information

Additional Supporting Information may be found online in the Supporting Information section at the end of the article:

Fig. S1 miR156-overexpressing tomato meristems transition to reproductive stage *c.* 30 d post-germination.

Fig. S2 Proper PROCERA/DELLA activity is required for flower induction in M82.

Fig. S3 miR156, *PRO/DELLA*, and *SINGLE FLOWER TRUSS* expression patterns in tomato.

Fig. S4 Expression of GA biosynthetic and catabolic genes at the tomato shoot apex.

Fig. S5 Two-hybrid system (Y2H) assays.

Fig. S6 miR319-targeted *LANCEOLATE* modulates meristem maturation.

Fig. S7 Inflorescence complexity is reduced in *La-1/+* plants.

Fig. S8 Expression patterns of miR319- and miR156-targeted *SISBP15* at the tomato shoot apex.

Fig. S9 Interplay between miR319-targeted *LANCEOLATE* and the miR156-*SISBP* module controls floral transition and inflorescence development in the hybrid background.

Fig. S10 Overexpression of the *SINGLE FLOWER TRUSS* (*SFT*) leads to early-flowering phenotype in ‘Micro-Tom’ (MT).

Fig. S11 Deregulation of miR319-targeted *TCP4* promotes flowering in *Arabidopsis*.

Fig. S12 M82 plants displayed early flowering after PAC treatment.

Fig. S13 PAC treatment promotes modifications in tomato vegetative development.

Table S1 Oligonucleotide sequences used in this work.

Please note: Wiley Blackwell are not responsible for the content or functionality of any Supporting Information supplied by the authors. Any queries (other than missing material) should be directed to the *New Phytologist* Central Office.